Postprint of: Parchem K., Baranowska M., Kościelak A., Kłosowska-Chomiczewska I., Domingues M. R., Macierzanka A., Bartoszek-Pączkowska A., Effect of oxidation and in vitro intestinal hydrolysis on phospholipid toxicity towards HT29 cell line serving as a model of human intestinal epithelium, FOOD RESEARCH INTERNATIONAL, Vol. 163 (2023), 112227, DOI: 10.1016/j.foodres.2022.112227

Effect of oxidation and *in vitro* intestinal hydrolysis on phospholipid toxicity towards HT29 cell line serving as a model of human intestinal epithelium

Karol Parchem[a]*, Monika Baranowska[a], Anna Kościelak[a], Ilona Kłosowska-Chomiczewska[b], Maria Rosário Domingues[c,d], Adam Macierzanka[b], Agnieszka Bartoszek[a]

[a] Department of Food Chemistry, Technology and Biotechnology, Faculty of Chemistry, Gdańsk University of Technology, 11/12 Gabriela Narutowicza St., 80-233 Gdansk, Poland, karol.parchem@pg.edu.pl or parchem.karol@gmail.com (K.P.) bbmmonik@gmail.com (M.B.) anna.koscielak@pg.edu.pl (A.K.), agnieszka.bartoszek@pg.edu.pl (A.B.)

[b] Department of Colloid and Lipid Science, Faculty of Chemistry, Gdańsk University of Technology, 11/12 Gabriela Narutowicza St., 80-233 Gdansk, Poland, ilona.chomiczewska@pg.edu.pl (I.K-C), adam.macierzanka@pg.edu.pl (A.M.)

[c] Mass Spectrometry Centre, LAQV-REQUIMTE, Department of Chemistry, University of Aveiro, Santiago University Campus, 3810-193 Aveiro, Portugal, mrd@ua.pt (M.R.D)

[d] Centre for Environmental and Marine Studies, CESAM, Department of Chemistry, University of Aveiro, Santiago University Campus, 3810-193 Aveiro, Portugal, mrd@ua.pt (M.R.D)

*Corresponding author:

E-mail address: karol.parchem@pg.edu.pl or parchem.karol@gmail.com (K. Parchem)

Declarations of interest: none

Color figures only in the *online* version

Abstract

Oxidation of food-derived phospholipids (PLs) can influence nutrient digestion and induce oxidative stress in gastrointestinal epithelium. In this study, hen egg yolk PL fraction was used to evaluate the effect of lipoxygenase (LOX)-induced PL oxidation on the hydrolysis of PLs catalyzed by pancreatic phospholipase A_2 (PLA_2) in the presence of bile salts (BSs). Then, PL/BS solutions containing native or oxidized PLs were used in *in vitro* intestinal digestion to assess the effect of PL oxidation and hydrolysis on the toxicity towards HT29 cell line. Based on the obtained results, we suggest that hexanal and (*E*)-2-nonenal, formed by the decomposition of PL hydroperoxides, inhibited PLA_2 activity. The cell exposure to simulated intestinal fluid (SIF) containing BSs decreased HT29 cell viability and significantly damaged cellular DNA. However, the genotoxic effect was reversed in the presence of all tested PL samples, while the protective effect against the BS-induced cytotoxicity was observed for native non-hydrolyzed PLs, but was not clearly visible for other samples. This can result from an overlap of other toxic effects such as lipotoxicity or disturbance of cellular redox homeostasis. Tacking into account the data obtained, it was proposed that the PLA_2 activity decline in the presence of PL oxidation products may be a kind of protective mechanism against rapid release of oxidized FAs characterized by high cytotoxic effect towards intestinal epithelium cells.

Key words: oxidized phospholipids; phospholipid hydrolysis; pancreatic phospholipase A_2; bile salts; intestinal oxidative stress;

Abbreviations: BS – bile salts; CLD – cytosolic lipid droplets; ER – endoplasmic reticulum; FA – fatty acid; FAME – fatty acid methyl ester; GPx2 – gastrointestinal glutathione peroxidase 2; GSH – glutathione; GSSG – glutathione disulfide; IC – inhibitory concentration IEC – intestine epithelial cell; LOH – lipid hydroxide; LOOH – lipid hydroperoxide; LOP – lipid oxidation products; LOX – lipoxygenase; LPL – lysophospholipid; MDA – malondialdehyde; O/W – oil-in water emulsion; oxPL – oxidized phospholipid; PC – phosphatidylcholine; PDI – polydispersity index; PE – phosphatidylethanolamine; PL – phospholipid; PLA_2 – phospholipase A_2; PUFA – polyunsaturated fatty acid; PV – peroxide value; RNS – reactive nitrogen species; ROS – reactive oxygen species; SFA – saturated fatty acid; SIF – simulated intestinal fluid; TAG – triacylglycerol; TBARS – thiobarbituric acid reactive substances; UFA – unsaturated fatty acid.

1. Introduction

Phospholipids (PLs) are important biomolecules, which apart from building cell and organelle membranes, also play a role of endogenous signalling molecules. The biophysical properties of membranes, including their fluidity and permeability as well as the distribution and activity of embedded proteins, are related to the composition of lipid bilayer, including PL structures or cholesterol to PL ratio (Küllenberg de Gaudry, Taylor, Schneider, & Massing, 2012). Moreover, polyunsaturated fatty acids (PUFAs) present in the structure of membrane PLs can be oxidatively modified under oxidative stress conditions. Such modifications change hydrophobicity of the fatty acids (FAs) build in the PL structure, which perturbs the assembly of the cellular membranes and alters their functional properties, e.g., by disturbing ion and nutrient transport (Catalá, 2012; Catalá & Díaz, 2016). Additionally, endogenous oxidized PLs (oxPLs) may be recognized by specific receptors leading to the activation of signaling pathways that mediate the inflammatory response or cell apoptosis (Fruhwirth, Loidl, & Hermetter, 2007). Therefore, elevated levels of cellular or plasma oxPLs are believed to be implicated in the pathogeneses of some diseases and disorders (Parchem, Sasson, Ferreri, & Bartoszek, 2019). The endogenous abundance of oxPLs increases i.a., under the conditions of cellular oxidative stress, which results from imbalance between the prooxidant and antioxidant systems, and consequently the excessive production of reactive oxygen and nitrogen species (ROS/RNS).

Diet is one of the most relevant factors that can modulate cellular and tissue levels of ROS/RNS. It has been demonstrated that an overload of nutrients, especially caused by high-fat or/and high-glucose diets can be implicated in the disruption of cellular redox homeostasis. One of the mechanisms involved in oxidative stress induced by high-energy-dense diets is lipotoxicity, which result from inadequate lipid storage capacity in adipose tissue and/or abnormal adipose tissue lipolysis (Montgomery, De Nardo, & Watt, 2019). This leads to chronically elevated levels of plasma non-esterified FAs and increased ectopic lipid deposition. As a consequence, lipotoxic cellular outcomes including endoplasmic reticulum (ER) stress, inflammation, mitochondrial dysfunction and finally cell apoptosis can occur (Montgomery et al., 2019). Diet-related oxidative stress may result in dysfunction of various gastrointestinal cell types such as hepatocytes (Lian, Zhai, Li, & Wang, 2020), pancreatic β-cells (Sasson, 2017) or intestine epithelial cells (IECs) (Gulhane et al., 2016). The latter can be exposed to overhigh FA concentration in both, basolateral and apical sides (Bashllari et al., 2020; Van

Rijn et al., 2019). Another factor that can trigger cellular oxidative stress is an exposition of IECs to food-delivered lipid oxidation products (LOPs) (Awada et al., 2012). PUFAs present in the structure of dietary lipids are highly prone to oxidative modifications during food processing and storage (Wąsowicz et al., 2004) as well as in the gastrointestinal digestion (Nieva-Echevarría, Goicoechea, & Guillén, 2018). Importantly, previous studies indicated that for foods such as fish or meat, oxidative changes first occurred in PLs and then in triacylglycerols (TAGs) (Igene, Pearson, Dugan, & Price, 1980; Jittrepotch, Ushio, & Ohshima, 2006). This order result from higher unsaturation of FAs in the structures of muscle PLs compare to TAGs from the same origin (Cui & Decker, 2016; Guyon, Meynier, & de Lamballerie, 2016). Additionally, it seams that PLs, due to their presence in cellular membranes characterized by large surface area, are more exposed to prooxidant molecules (Cui & Decker, 2016).

PLs, next to bile salts (BS), are surface-active compounds that facilitate solubilization of ingested oils and fats, leading to the formation of an oil-in water (O/W) emulsion. As a result of pancreatic lipolytic enzyme activity, dietary lipids are hydrolyzed, and the formed products are removed form the O/W surface. However, the presence of oxidized (phospho)lipids in the colloidal structures subjected to intestinal digestion can change the kinetics of lipolysis. So far, this topic has only been covered in few research studies. For example, Baba et al., observed that porcine pancreatic PLA_2 preferentially released 13(S)-hydroperoxy-(9Z,11E)-octadecadienoic acid from the *sn*-2 position of phosphatidylcholine (PC) molecule in the presence of sodium deoxycholate compared to non-oxidized PC species (Baba, Mikami, Shigeta, Nakajima, & Matsuo, 1993). In another study, the authors monitored the activity of porcine pancreatic PLA_2 towards UV-irradiated hen egg yolk PC species in PC/sodium deoxycholate mixed micelle structures compared to the non-irradiated sample (Litvinko, Skorostetskaya, & Gerlovsky, 2018). The obtained data revealed the increase in the rate of PLA_2-catalyzed hydrolysis of PC fraction exposed up to 40 min to the UV-irradiation, while after this time the enzymatic activity declined. It was suggested that the presence of primary product of PC oxidation (PC hydroperoxides) lead to PLA_2 activation and efficient removal of oxidatively modified FA from the PC structure. After 40 min of PC irradiation, a significant increase in malondialdehyde (MDA) level was observed. Probably, MDA and other highly reactive secondary lipid oxidation products were responsible for the inhibition of PLA_2 activity (Litvinko et al., 2018).

As mentioned earlier, increased absorption and accumulation of oxidized lipids and products of their

decomposition, such as 4-hydroxy-2-alkenals, by IECs can contribute to the disruption of cellular redox homeostasis. However, exposure of human colon adenocarcinoma Caco-2/TC7 cells to a relatively low LOP concentration has been shown to induce cellular antioxidant systems including overexpression of gastrointestinal glutathione peroxidase 2 (GPx2) (Awada et al., 2012). This enzyme is responsible for detoxification and degradation of hydrogen peroxide (H_2O_2) and lipid hydroperoxides (LOOHs) to water and lipid hydroxides (LOH), respectively (Awada et al., 2012). Elevated LOP concentration and/or chronic cell exposure to these products can disrupt cellular antioxidant systems. The previous *in vivo* study in rats indicated that chronic exposure to subtoxic level of oxidized fish oil led to a decrease in the intestinal tissue glutathione (GSH) in favour of glutathione disulfide (GSSG) concentration (Tsunada et al., 2003). Moreover, the disturbance of intestinal GSH/GSSG ratio resulting from cell exposure to oxidized lipids, induced cellular transitions from proliferation to growth arrest and apoptosis (Tsunada et al., 2003). This example clearly indicated the effects of redox imbalance on intestinal cell dysfunction.

The main cellular structures that can by modified due to oxidative stress include membrane lipids, proteins and nucleic acids. Concerning ROS-induced modifications of (phospho)lipids, these include hydroxylation, peroxidation or carbonylation of unsaturated FAs (UFAs) as well as the cleavage of the C-C bond along FA acyl chain to form truncated (phospho)lipids (T. Y. Wang, Libardo, Angeles-Boza, & Pellois, 2017). Such oxidative alterations of UFAs present within membrane PLs prevent their immersion in the interior of the bilayer and lead to the translocation of oxidized FAs onto membrane surface in the form of so-called “whiskers” (Catalá, 2015). The accumulation of such aberrant structures can alter plasma, mitochondrial or ER membrane properties and thus their functions. Therefore, the modified membranes require reconstruction to maintain their original biophysical and functional properties. Oxidatively modified acyl chains of membrane PLs can be removed from the backbone upon hydrolysis catalyzed by intracellular or plasma phospholipases A_2 (PLA_2) (Fruhwirth et al., 2007), followed by re-acylation of membrane PLs to restore their original structure. It has been suggested that the dynamic pool of undamaged UFAs for the membrane PL re-synthesis is provided by cellular TAGs stored in cytosolic lipid droplets (CLDs) (Girón-Calle, Schmid, & Schmid, 1997; Pamplona, 2008). The accumulation and FA composition of TAGs in CLDs strictly depend on the amount and the type of ingested lipids, especially in the case of IECs. The products of the intestinal lipolysis are re-synthesized to TAGs or PLs at the ER membrane after their absorption by enterocytes.

Next, in the ER lumen, the formed lipids are used for assembling of chylomicrons, which are finally secreted *via* lymphatic system to bloodstream (Beilstein, Carrière, Leturque, & Demignot, 2016). In order to avoid postprandial hypertriglyceridemia, the re-synthesized lipids may be temporary stored in the CLDs of enterocytes. In this period, enterocytes can hydrolyze esterified lipids and use the released FAs for their own needs e.g., energy production or membrane biosynthesis. In the interprandial phase, the storage lipids can be mobilized for chylomicron formation (Beilstein et al., 2016).

Another way of repairing damaged cellular membranes implies a direct incorporation of orally administrated PLs into cellular lipid bilayers. Such an approach, called lipid replacement therapy was proposed by Nicolson and involves a delivery of PLs to tissues and cells with limitations of their oxidation during the storage, ingestion, digestion and uptake as well as prevention of the intestinal hydrolysis of orally-administered PLs (Nicolson & Ash, 2014). Interestingly, some literature data indicated that even 20 % of dietary PLs can be absorbed by enterocytes in undigested form (Küllenberg de Gaudry et al., 2012) and potentially directly affect the membrane lipid remodelling. However, most of the consumed PLs are hydrolyzed in the small intestine by pancreatic phospholipase A_2 (PLA_2) to lysophospholipids (LPLs) and FAs and then re-synthesized at the ER membrane.

Food-delivered PLs are known for their high nutritional value and beneficial health effects, not only as a source of essential FAs, but also due to their anti-inflammatory, antioxidant, antifibrogenic, membrane-protective and lipid-regulating properties (Blesso, 2015; Gundermann, Gundermann, Drozdzik, & Mohan Prasad, 2016; Küllenberg de Gaudry et al., 2012). However, PLs, especially those rich in PUFAs, are susceptible to oxidative modifications during the food processing and storage as well as the gastrointestinal digestion. Nevertheless, to date, data on the influence of PL oxidation on their intestinal digestion and the biological effect of the resulting products on IECs are limited. Therefore, in our study, we proposed several research models to understand step-by-step the role of PL oxidation and intestinal hydrolysis on IEC physiology and pathophysiology. The aim of this study was threefold: (i) to evaluate the effect of lipoxygenase (LOX)-induced oxidative modification of egg yolk PL fraction on the parameters of colloidal structure found in the simulated *in vitro* intestinal fluid containing bile salts (BSs); (ii) to determine the effect of PL oxidation on the kinetics of their *in vitro* intestinal hydrolysis catalyzed by pancreatic PLA_2 in the presence of BSs, and (iii) to assess the

impact of native and oxidized PLs, both before and after *in vitro* intestinal hydrolysis, on HT29 cell physiology, serving as a model of intestinal tissue exposed to direct contact with ingested food ingredients. This cell line is a human intestinal epithelial cell line derived from human colorectal adenocarcinoma. However, HT29 cells express features of both absorptive enterocytes and intestinal secretory cells producing a gelatinous mucus-like substance (Fedi et al., 2021). Additionally, its differentiated phenotype is similar to small intestine enterocytes in terms of their structure and the presence of brush border-associated hydrolases (Martínez-Maqueda, Miralles, & Recio, 2015). Therefore, this cell line has been widely used in *in vitro* studies of cellular absorption, bioavailability and metabolism of food molecules (Martínez-Maqueda et al., 2015). Nevertheless, it should be noted that this cellular model has some disadvantage arising from cancerous and non-small intestinal origin, therefore differences in the gene expression of transporters and metabolic enzymes can be observed compare to the normal small intestinal cells (Fedi et al., 2021; Martínez-Maqueda et al., 2015). However, the aim of this research was to evaluate the effect of PL oxidation and hydrolysis on physiology of IECs and understanding the mechanism of toxicity of formed products, therefore we found this model to be appropriate.

2. Materials and methods

2.1. Chemicals and materials

Acetic acid, acetone, chloroform, hexane, methanol, ethanol (96 %), boric acid, disodium tetraborate decahydrate, sulphuric acid, hydrochloric acid (HCl), potassium iodine, sodium thiosulfate, sodium chloride (NaCl), calcium chloride ($CaCl_2$), 2-amino-2-(hydroxymethyl)-1,3-propanediol (Tris-base), 0.1 M sodium hydroxide solution (NaOH), ethylenediaminetetraacetic acid (EDTA) (all ACS grade) and acetonitrile (HPLC gradient grade) were purchased from Merck KGaA (Darmstadt, Germany). Ammonium formate (LC-MS grade) was obtained from VWR International (Leicestershire, UK). Lipoxidase from *Glycine max* (soybean) type I-B (LOX-1), sodium deoxycholate (≥98%), molybdenum (≥99.9), molybdenum (VI) oxide (≥99.9), fatty acid methyl ester (FAME) standards, trichloroacetic acid (TCA), thiobarbituric acid (TBA), butylated hydroxytoluene (BHT), olive oil highly refined, bile salt (BS) mixture (United States Pharmacopeia Reference Standard), pancreatic phospholipase A_2 (PLA_2), Varespladib (≥98%), thiazolyl blue tetrazolium bromide (MTT), dimethyl sulfoxide (DMSO), tablets of phosphate buffered saline (PBS), low melting point agarose (LMP agarose), Sybr Green I nucleic acid gel stain, Triton X100, formaldehyde, Nile Red were derived from Sigma-Aldrich, Merck KGaA

(Darmstadt, Germany). Normal melting point agarose (NMP agarose) was obtained form Bioline (London, United Kingdom). High purity water was produced using Millipore Elix 5 purification system (Darmstadt, Germany). Fresh free-range hen eggs with a mass in the range of 63-73 g were purchased in a local market (Gdansk, Poland).

2.2. Study design

PL fraction was isolated from fresh hen eggs and its composition was characterized by chromatography taking into account PL classes and FA composition (Fig. 1). In order to determine the effect of oxidative modification of PL on the kinetics of their hydrolysis and potential toxicity towards intestinal cells, part of the native PL fraction was enzymatically oxidized by LOX. The degree of PL oxidation was assessed by determination of peroxide value (PV) and thiobarbituric acid reactive substances (TBARS). In the next step, native and oxidized PLs were used to prepare aggregation structures (mixed micelles solutions and emulsions) in simulated intestinal fluid (SIF) containing BS whose concentration matched physiological levels. The BS concentration in the prepared solutions was calculated based the average molecular mass of commercially available BS mixture (c.a. 519.0 g/mol) and was about 9.6 mM. While the physiological BS concentration in the postprandial state range from 4 – 20 mM (Maldonado-Valderrama, Wilde, MacIerzanka, & MacKie, 2011). The obtained aggregation structures were characterized in terms of size distribution and dispersity and then subjected to *in vitro* intestinal digestion. The kinetics of PL hydrolysis catalyzed by porcine pancreatic PLA_2 was monitored using pH-stat titration (pH=8). The samples of native and oxidized PL/BS mixed micelle solutions before and after hydrolysis were then used for comparisons of their biological effects. One of the cell lines recommended by the Replacement, Refinement and Reduction of Animals in Research for nutritional studies is HT29 (human colon adenocarcinoma) cell line, which was employed in this study (Krishna & Gopalakrishnan, 2016). The PL/BS mixed micelle solutions were added to cell culture medium in the amount of 10 % *v/v*. The impact of PL oxidation and hydrolysis on cell physiology was evaluated by determination of cell viability by MTT test, genotoxicity by comet assay and ability of cells to neutral lipid accumulation using fluorescence microscopy.

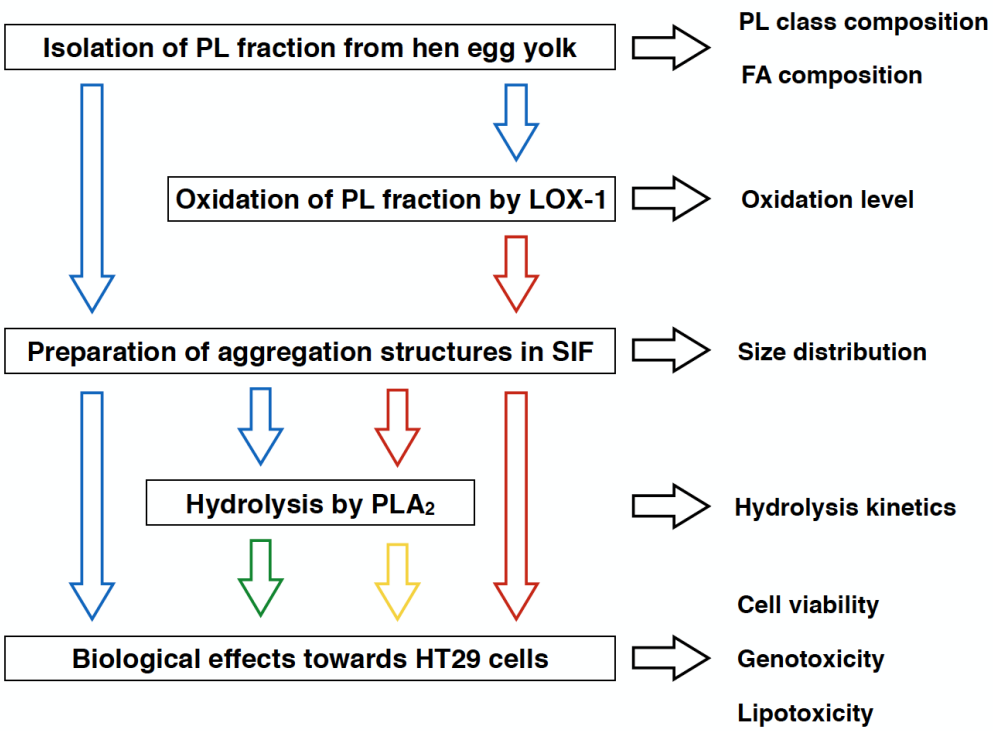

Fig. 1. Study design. (Abbreviations: FA – fatty acid; LOX-1 – lipoxygenase type 1; PL – phospholipid; PLA_2 – phospholipase A_2; SIF – simulated intestinal fluid)

2.3. Isolation of hen egg yolk PL fraction

Hen egg yolk PL fraction was isolated as described previously by Gładkowski et al. (Gładkowski, Chojnacka, Kiełbowicz, Trziszka, & Wawrzeńczyk, 2012) with further modifications (Parchem, Kusznierewicz, Chmiel, Maciołek, & Bartoszek, 2019). Briefly, two egg yolks were combined with 120 mL of methanol, stirred for 10 min and left at room temperature until the alcohol-insoluble fraction precipitated. Then, the supernatant was filtered and the precipitate was re-extracted twice with 120 mL of methanol. The extracts were combined and the solvent was evaporated under reduced pressure at 40 °C using a rotary evaporator. The residue was dissolved in 20 mL of hexane and transferred to a glass flask placed in an ice bath. Afterwards, under constant stirring, 120 mL of cold acetone at −20 °C was carefully added until PL fraction precipitated. The precipitate was then carefully washed 3 times with 40 mL of cold acetone at −20 °C and the solvent was removed each time by decantation. Finally, the PL fraction was dried in a stream of nitrogen, frozen overnight at −20 °C and freeze-dried for 48 h using laboratory freeze dryer Alpha 1-4 (Christ, Germany). The samples were stored at −80 °C in nitrogen atmosphere until used for experiments.

2.4. Lipoxygenase-catalyzed oxidation of egg yolk PLs

The enzymatic peroxidation was carried out as described previously by Butler O'Connor et al. (Butler O'Connor et al., 2010) with further modifications (Parchem, Kusznierewicz, et al., 2019). The methanolic solution of egg yolk PL fraction (20 mg/mL) was perpetrated in a round bottom flask. Methanol was evaporated under reduced pressure at 40 °C using a rotary evaporator and the PL fraction was dried at room temperature for 1 h in a stream of nitrogen. The obtained PL film was then hydrated with borate buffer (0.2 M, pH=9) containing 10 mM sodium deoxycholate. Prior to the addition of bile salt, the buffer was saturated with oxygen at room temperature for 30 min. Enzymatic peroxidation of PL was initiated by adding freshly prepared soybean lipoxidase type 1 (LOX-1) solution in the borate buffer. The final PL concentration was 5 mg/mL and the LOX-1 activity was 70 kU/mL. The reaction was carried out at 37 °C under oxygen atmosphere for 1 h. The peroxidation was stopped by the addition of chloroform/methanol mixture (2:1 *v/v*) in a volume equal to the volume of the reaction mixture. After intense shaking, the mixture was distributed to glass tubes and centrifuged (1600 × *g*, 5 min). The upper organic layer was transferred with a glass Pasteur pipettes to a round bottom flask. Then, the solvent was evaporated under a stream of nitrogen at 40 °C, frozen overnight at −20 °C, followed by freeze-drying for 48 h using laboratory freeze dryer Alpha 1-4 (Christ, Germany). The samples were stored at −80 °C in nitrogen atmosphere for further experiments.

2.5. Characterization of egg yolk PL fraction

2.5.1. Chromatographic analysis of PL classes

Hen egg yolk PL classes were analyzed using hydrophilic interaction liquid chromatography (HILIC) as described previously by Lisa et al. (Lísa, Cífková, & Holčapek, 2011) with further modifications (Parchem, Kusznierewicz, et al., 2019). The separation of individual PL classes was performed using a Dionex UltiMate 3000 LC system (Thermo Scientific, USA) equipped with a Rx-SIL column (250 × 4.5 mm, 5 µm) (Agilent Technology, USA). The mobile phase consisted of acetonitrile (A) and 5 mM aqueous ammonium formate (B). The gradient program was as follows: 0 – 30 min, 6 – 77 % B, 30 – 35 min, 77 % B, finally the column was re-equilibrated to the initial conditions for 20 min. The separation was carried out at of 40 °C with a flow rate of 1 mL/min. The injection volume was 20 µL. The eluted PL classes were monitored using a Corona Ultra RS CAD (Thermo Scientific, USA) with following parameters: acquisition range of 100 pA, digital filter set to "none", gas flow (air) of 12 L/min and nebulizer pressure of 35 psi. Individual PL classes were identified by comparison of their retention times with those of standards (more details: (Parchem, Kusznierewicz, et al., 2019)). Results are

expressed as a mean of three independent determinations of the percentage of the individual PL classes in total PLs identified in the sample.

2.5.2. Analysis of FA composition in the structure of PC and PE fractions

The methanolic solution of PLs (20 mg/mL) in a volume of 100 µL was applied onto a preparative TLC glass silica gel plate (20 × 20 cm, 1 mm, 10-12 µm) (Merck, Germany) as a 20 cm band using a hand-held applicator equipped with a 100 µL syringe. PL classes were separated with chloroform/methanol/acetic acid/water mixture (35:25:4:14:2 v/v/v/v) (Palusinska-Szysz, Kania, Turska-Szewczuk, & Danikiewicz, 2014). After separation, the plate was dried using a stream of nitrogen and sprayed with a molybdenum reagent (Dittmer & Lester, 1964) over a width of 2 cm in order to locate individual PL classes. Then, silica gel from areas corresponding to the two main PL classes present in egg yolk (PCs and phosphatidylethanolamines (Pes)) was scraped off from the non-sprayed part of the plate using metal spatula. PC and PE fractions were extracted from the appropriate portions of silica gel using 10 mL of chloroform/methanol (2:1 *v/v*) mixture. The extraction was repeated twice. The obtained extracts corresponding to individual PL classes were combined and the solvent was evaporated under reduced pressure at 40 °C using rotary evaporator.

Fas present in the structure of PCs and Pes were esterified to fatty acid methyl esters (FAMEs) according to the European Standard [EN:ISO 5509:2000]. FAMEs were analyzed using high-performance gas chromatography (HP-GC). The separation of FAMEs was performed using Perkin Elmer Autosystem XL gas chromatograph (Perkin Elmer, USA) equipped with split injector 60:1 and CP-Sil 88 column (50 m × 0,25 mm × 0,2 µm, Agilent Technology, USA). FAMEs were detected using flame ionization detector (FID). The injector and FID temperatures were maintained at 250 °C. The initial column temperature was 170 °C and held for 30 min, followed by an increase of 10 °C/min up to 200 °C and held for 15 min. Finally, the temperature was raised to 210 °C at a rate of 5 °C/min and held for 10 min. Qualitative and quantitative analyses of Fas in the samples were performed using FAME standards. Results are expressed as means of three independent determinations of the percentage of the individual Fas in total Fas identified in the sample.

2.5.3. Determination of peroxide value of PL fraction

The peroxide value (PV) of native and oxidized PL fractions was determined according to the method described previously (Fruehwirth et al., 2020) with some modifications. The appropriate amount of PL

fraction (1 g and 50 mg for native and oxidized PL fraction, respectively) was dissolved in 5 mL of acetic acid/chloroform (3:2 *v/v*) mixture. The differences in weighted amounts between the native and oxidized samples resulted from a significant difference in the content of PL hydroperoxides. Therefore, the sample amount was optimized such that the volume of titrant added was between 2 and 18 mL using a 20 mL burette. Then, 200 µL of a saturated potassium iodide solution was added, the sample was shaken for 1 min and placed in darkness for 5 min. Afterwards, 15 mL of distilled water and few droplets of 1 % *w/w* starch solution were added. The samples were titrated using 0.002 N sodium thiosulfate solution until complete discoloration was reached. The blank test was performed without PL fraction. The samples were analyzed in triplicate.

2.5.4. Determination of TBARS content

The amount of thiobarbituric acid reactive substances (TBARS) in native and oxidized PL fraction was determined by method described by Fenaille et al. (Fenaille, Mottier, Turesky, Ali, & Guy, 2001) with modifications. In brief, 1 mL of aqueous solutions of PL fraction (10 and 2.5 mg/mL for native and oxidized PL fraction, respectively) was combined with 1 mL of reaction mixture containing equal volumes of 15 % trichloroacetic acid (TCA), 0.25 M HCl and 0.375 % thiobarbituric acid (TBA), followed by the addition of 0.1 mL of 0.4% solution of butylated hydroxytoluene (BHT) in 96% ethanol. The differences in weighted amounts between the native and oxidized samples resulted from a significant difference in the content TBARS. Therefore, the sample amount was optimized such that the absorbance was below 1.5 as recommended by manufacturer. The sample was shaken for 1 min and then centrifuged (4700 × *g*, 5 min). The supernatant was collected to the new tube, while the precipitate was mixed with another 1 mL of reaction mixture, shaken and centrifuged. The combined supernatants were incubated at 95 °C under nitrogen atmosphere for 30 min. Then, the reaction was stopped by cooing the sample in an ice bath. The mixture was made up to 12 mL with distilled water and centrifuged (4700 × *g*, 5 min). The absorbance of the supernatant was measured at wavelengths of 532 and 600 nm as a background. The TBARS content was calculated based on molar extinction coefficient (ε) for MDA-TBA_2 adduct (1.55×10^5 $M^{-1} \times cm^{-1}$) (Meca et al., 2021). The samples were analyzed in triplicate.

2.6. Preparation and characterization of PL/BS mixed micelles and PL/BS/TAG emulsions

The PL/BS mixed micelle solution was prepared by dispersing 1 % *w/v* egg yolk PL fractions in the simulated intestinal fluid (SIF) containing 150 mM NaCl, 6 mM $CaCl_2$, 0.28 mM Tris-base and 5 mg/mL of BS mixture. The composition of used BS mixture is shown in Supplementary Materials (Table A1). The solution was then sonicated on ice (20 kHz, 4 min) to reduce the particle size and to homogenize the mixed micelles using Vibra-Cell VC 750 ultrasound sources fitted with a 3 mm diameter titanium micro-tip VCX500 (Sonics, USA). Power delivery was controlled as amplitude percentage, which was set as 40 %. A pulsed duty cycle of 8 sec on and 2 sec off was used for all experiments. The PL/BS/TAG emulsion was prepared by dispersing 1 % *w/v* egg yolk PL fractions and 1.5 % *w/v* highly refined olive oil in SIF. The solution was then sonicated using the conditions outlined above.

The mixed micelle and emulsion droplet size distribution and dispersity (polydispersity index, PDI) were determined using a non-invasive black scatter (NIBS) technique (Kupper, Kłosowska-Chomiczewska, & Szumała, 2017). For this purpose, a Zetasizer Nano ZS (Malvern, United Kingdom) equipped with a helium-neon laser diffraction operating at 633 nm was employed. For the mixed micelles, the samples were analyzed directly without dilution, while the emulsion samples were diluted with the buffer (150 mM NaCl, 6 mM $CaCl_2$, 0.28 mM Tris base, pH=8) in a ratio of 1:1000. All measurements were performed at 37 °C. The samples were analyzed in quintuplicate.

2.7. *In vitro* intestinal PL hydrolysis

Four digestive systems, consisting of native or oxidized PL fraction without or with TAGs, have been proposed to understand the effect of PL oxidation and the aggregation structure in which PL are embedded on kinetics of their hydrolysis catalyzed by PLA_2. The kinetics of PL hydrolysis was monitored using a pH-stat method, in which enzymatically released Fas were continually titrated with 0.1 M NaOH to keep the pH constant at 8.0. The mixed micelle solution or emulsion in the volume of 15 mL was placed in a titration vessel of the T70 titrator (Mettler Toledo, USA). The sample was pre-incubated at 37 °C for 15 min until the temperature equilibration and then pH value was adjusted to 8.0 using 0.1 M NaOH and 0.1 M HCl. The reaction was initiated by the addition of porcine pancreatic phospholipase A_2 (PLA_2) to reach the final activity of 35 U/mL. The PL hydrolysis was carried out at 37 °C with continuous stirring (40 % of the maximum stirring speed). Unless otherwise stated, the hydrolysis reaction was carried out for 1 h. Hydrolysis reactions were carried out in triplicate for each sample type.

2.8. PLA_2 activity in the presence of aldehydes

The native PL/BS mixed micelles solution was prepared as described in section 2.6. The samples was placed in the titration vessel of the T70 titrator (Mettler Toledo, USA) and pre-incubated at 37 °C for 15 min. Then, appropriate volumes of low-molecular aldehydes (hexanal or €-2-nonenal), corresponding to the following final concentrations: 0, 5, 10, 15, 20 mM, were added. For this range, a negative linear correlation was observed between the concentration of tested aldehydes and the PLA_2 activity, which allowed for determination of IC_{10} and IC_{30} values. The pH value was adjusted to 8.0 followed by addition of porcine pancreatic PLA_2) with the final activity of 30 U/mL. PLA_2 activity was calculated based on the volume of 0.1 M NaOH added after 20 min from the start of the reaction according to the Eq. 1.

$$PLA_2\ activity = (V_{NaOH} \times c_{NaOH}) / t \quad \text{(Eq.1)}$$

where:

$PLA_2\ activity$ – phospholipase A_2 activity [mol of FA released/min],

V_{NaOH} – volume of consumed NaOH solution [dm^3],

c_{NaOH} – concentration of used NaOH solution [mol/dm^3],

t – hydrolysis time [min].

Hydrolysis reactions were carried out in triplicate for each concentration points for both aldehydes.

2.9. Cell culture

HT29 (human colon adenocarcinoma) cell line was purchased from American Type Culture Collection (ATCC). The HT29 cells were maintained in the McCoy's 5A medium supplemented with fetal bovine serum (100 mL/L) and antibiotics: penicillin (100 g/L) and streptomycin (100 U/mL). All reagents for cell culture were purchases from Sigma-Aldrich, Merck KgaA (Darmstadt, Germany). The cells were cultured at 37 °C under humidified atmosphere containing 5% CO_2 in a cell incubator (Heal Force, China). For the experiments, the cells derived from passages between 6 and 11 were used. The cells were regularly tested for mycoplasma contamination using Universal Mycoplasma Detection Kit from ATCC.

2.9.1. Preparation of native and oxidized PL/BS mixed micelle solution for cell treatment

The solutions of native and oxidized PL in SIF (native and oxidized PL/BL mixed micelles) were prepared just before cell treatment. In the case of non-hydrolyzed PL, the samples were incubated in 37 °C without addition of PLA_2, while the digested samples were subjected to hydrolysis catalyzed by PLA_2 (Section 2.7). For the cell treatment purposes, the hydrolysis reaction was stopped after releasing 40 % of the Fas present at the *sn*-2 position of glycerol backbone. Based on the hydrolysis reaction stoichiometry and taking into account the average molecular mass of egg yolk PL (c.a. 752.3 g/mol), the mentioned PL hydrolysis degree was achieved after adding 0.8 mL of 0.1 M NaOH solution during pH-stat titration. The PL hydrolysis was terminated by the addition of secretory PLA_2 inhibitor – Varespladib (Dennis, Cao, Hsu, Magrioti, & Kokotos, 2011). Based on the preliminary study, Varespladib at the concentration of 5 μM was found to be appropriate for the complete inhibition of porcine pancreatic PLA_2. For this purpose, 15 μL of 5 mM Varespladib dissolved in DMSO was added to 15 mL of digestion mixture. To eliminate the differences between samples, this inhibitor was added to non-hydrolyzed samples as well. Additionally, the effect of Varespladib alone on the viability of HT29 cells was determined. The cells were treated with inhibitor at the concentration of 0.5 μM (the final concentration in cell culture medium after addition digestion mixtures in the proportion 9:1. The treatment was carried out for 6, 24, 48 and 72 h. To obtain the PL solutions with different concentrations, non-hydrolyzed and hydrolyzed samples were diluted using SIF (150 mM NaCl, 6 mM $CaCl_2$, 0.28 mM Tris-base, 5 mg/mL BS, pH=8) containing 5 μM Varespladib. The final concentrations of PLs and products of their hydrolysis (LPLs and Fas) in individual samples are shown in **Supplementary Materials (Table A2)**.

2.9.2. Determination of cytotoxicity towards HT29 cells by MTT test

To determined the effect of native and oxidized PL before and after hydrolysis on cell viability, the MTT test was applied as described previously (Baranowska et al., 2018, 2020, 2021). In brief, the exponentially growing HT29 cells were seeded in 96-well cell culture plates (5×10^3 cells per well in 180 μL of medium) and were allowed to settle for 24 h at 37 °C under 5 % CO_2 atmosphere. Then, the cells were treated for 6, 24, 48 and 72 h with 20 μL of different concentrations of native or oxidized PL, before or after *in vitro* intestinal hydrolysis (Table A2). Control cells were treated with the buffer (150 mM NaCl, 6 mM $CaCl_2$, 0.28 mM Tris-base, pH=8) or SIF (containing 5 mg/mL of BS mixture). After 6, 24, and 48 h of exposure, the medium was aspirated from the wells and replaced with 200 μL of fresh medium. Then, the cells were incubated at 37 °C under 5 % CO_2 until 72 h of the total incubation time.

For the 72 h exposure, the medium was replaced for fresh one at the endpoint. After treatment, 50 µL of MTT solution (4 g/L) was added to all wells and the cells were incubated for another 4 h at 37 °C under 5 % CO_2. Finally, the medium was carefully removed from wells and the formazan crystals formed by metabolically active cells were dissolved in 50 µL of DMSO. The absorbance of the obtained solutions was measured at wavelength of 540 nm and a reference wavelength 690 nm using TECAN Infinite M200 plate reader (Tecan Group Ltd., Switzerland). The differences in absorbance between formazan specific A_{540} and the background A_{690} for individual wells were used for further calculations. Cell treatments were performed as four technical repetitions and three independent repetitions. Cytotoxic effect of tested lipids was expressed as per cent of cell viability compared to control cells treated for 6, 24, 48 or 72 h with 20 µL of the buffer (150 mM NaCl, 6 mM $CaCl_2$, 0.28 mM Tris-base, pH=8) containing 5 µM Varespladib (final concentration in culture medium was 0.5 µM), whose viability was regarded as 100 %. The second type of control constituted cells treated for 6, 24, 48 or 72 h with 20 µL of SIF with 5 mg/mL of BS mixture containing 5 µM Varespladib. Results are expressed as means of three independent experiments carried out as four technical replicates.

2.9.3. Determination of genotoxic effect by comet assay

To determine the genotoxic effect of native and oxidized PL before and after hydrolysis in HT29 cells, the comet assay was applied as described previously (Baranowska et al., 2018, 2020, 2021). Briefly, the exponentially growing HT29 cells were seeded in 24-well cell culture plates (10^5 cells per well in 1.8 mL of medium) and were allowed to settle for 24 h at 37 °C under 5 % CO_2 atmosphere. Then, the cells were treated for 24 h with 200 µL of two concentrations of native or oxidized PL, before or after *in vitro* intestinal hydrolysis (125 and 250 µg/mL) (Table A2). After exposure, the medium was aspirated from the wells and the cells were washed with 0.5 mL of cold PBS, followed by cell detachment with 0.2 mL of trypsin solution (0.5 g/L). The addition of 1.8 mL of fresh medium to wells stopped the enzymatic activity of trypsin. Then, 1 mL portions of the cell suspensions were transferred into 1.5 mL tubes and centrifuged (100 × *g*, 5 min, 4 °C). The cell pellets were washed with 1 mL of cold PBS and centrifuged again. PBS was discarded and the cells were resuspended in 150 µL of 0.5 % low-melting point (LMP) agarose. Then, 40 µL of the cell suspension was placed as two spots on a microscope slides covered with normal-melting point (NMP) agarose. The slides were covered with coverslips and placed on an ice-cold tray for at least 5 min to solidify the agarose. After overnight lysis in a high salt alkaline buffer (2.5 M NaCl, 0.1 M EDTA, 10 mM Tris, 1 % Triton X100, pH 10), the slides were placed

on a Bio-Rad subcell GT electrophoresis platform (Bio-Rad UK), covered with cold electrophoresis buffer (0.3 M NaOH, 1 mM EDTA, pH 13) and chromatin was allowed to unwind for 25 min. Then, the electrophoresis was conducted at 26 V (0.75 V/cm) and 300 mA for 30 min in darkness at 4-8 °C. The slides were transferred to the neutralizing buffer (0.4 M Tris, pH 7.5) for 5 min. This step was repeated twice, then the slides were washed using distilled water and fixed in 70 % ethanol. The DNA was stained using SybrGreen in TE buffer (0.1 Tris-base, 1 mM 1 mM EDTA, pH 10) for 30 min. After staining, the slides were washed in distilled water for 5 min. Finally, the DNA comets were analyzed using fluorescence microscopy (Zeiss ImagerZ2, USA) coupled with a computerized slide scanning system (Metafer4, Germany). Comet analysis involved counting 200 consecutive nuclei per sample. Three slides with two repetitions on each were prepared for each concentration of tested lipid mixture. Genotoxicity of analyzed samples was expressed as the % of DNA in the comet tail relative to total cellular DNA. The control cells were treated for 24 h with 200 µL of the buffer (150 mM NaCl, 6 mM $CaCl_2$, 0.28 mM Tris-base, pH=8) containing 5 µM Varespladib (final concentration in culture medium was 0.5 µM) or SIF with 5 mg/mL of BS mixture containing 5 µM Varespladib. As the positive control served the cells exposed to 150 µM hydrogen peroxide for 1 h.

2.9.4. Visualization of cytosolic lipid droplets

To determine the ability of HT29 cells to accumulate neutral lipids, the cytosolic lipid droplets (CLDs) were visualized according to the method described earlier (Listenberger & Brown, 2007). The exponentially growing cells were seeded in 6-well cell culture plates (4×10^5 cells per well in 3.6 mL of medium) on the bottom of which, the sterile 22 × 22 mm coverslips were placed beforehand. The cells were allowed to settle for 24 h at 37 °C under 5 % CO_2 atmosphere. Then, the cells were treated for 24 h with 400 µL of 125 µg/mL test solutions containing native or oxidized PL, before or after *in vitro* intestinal hydrolysis (Table A2). After incubation time, the medium was aspirated from the wells and the cells were washed twice with 2 mL of cold PBS. Then, 2 mL of 4 % formaldehyde in PBS was added to wells and the cells were fixed for 30 min at room temperature. Next, the cells were washed twice with 2 mL of PBS. Immediately before CLD staining, 1 µL of Nile Red stock solution (1 mg/mL) in DMSO was diluted in 10 mL of 150 mM NaCl solution. Next, 1 mL of diluted Nile Red solution was added to all wells. The plates were kept in darkness for 10 min in room temperature, followed by cell washing three times with 2 mL of PBS each. In the next step, the coverslips were mounted onto glass slides using 30 µL of ProLong™ Diamond antifade mountant. Finally, the cytosolic lipid droplets were

visualized using fluorescence microscopy (Zeiss ImagerZ2, USA). The control cells were treated for 24 h with 400 µL of the buffer (150 mM NaCl, 6 mM $CaCl_2$, 0.28 mM Tris-base, pH=8) containing 5 µM Varespladib (final concentration in culture medium was 0.5 µM) or SIF with 5 mg/mL of BS mixture containing 5 µM Varespladib.

2.10. Statistical analysis

Results are expressed as means ± standard deviation (SD) values of three independent experiments unless otherwise stated. An unpaired Student's t-test ($p \leq 0.05$) was used to assess the statistical significance of FA composition in PC and PE fractions, PVs and TBARS contents in native and oxidized PL fractions. The statistical significance of the PLA_2-catalysed PL hydrolysis rate in different systems and Comet assay results was examined using one-way ANOVA with Tukey's post hoc test. The statistical analysis was performed using the Prism 6.0 software package (GraphPad Software, Inc., USA).

3. Results

3.1. Characterization of native and oxidized egg yolk PL fractions

3.1.1. PL class composition

A high purity PL fraction was obtained from hen egg yolk by methanol extraction followed by precipitation of PLs in acetone cooled to −20 °C. The obtained PL fraction contained approximately 5 % of non-PL compounds, such as TAGs, Fas and cholesterol, based on total peak areas determined during HILIC-CAD analysis. The same technique confirmed that the most abundant PL classes in hen egg yolk were PCs and Pes, whose amounts were 52.9 % and 30.4 % of total PLs, respectively (Table 1). Other PL classes identified were phosphatidylinositols (Pis) and phosphatidylglycerols (PGs), constituting approximately 5 % of total PLs. LPLs, namely lysophosphatidylcholines (LPCs) and lysophosphatidylethanolamines (LPEs) abundance amounted to 2.0 % and 1.5 % of total PLs, respectively. Additionally, sphingomyelins (SMs) were detected in hen egg yolk in the amount of 2.7 % of total PLs.

Table 1. Composition of PL classes present in PL fraction isolated from hen egg yolk.

PL class (abbreviation)	Composition [% of total peak areas]*
Lysophosphatidylethanolamines (LPEs)	1.54 ± 0.21
Lysophosphatidylcholines (LPCs)	2.03 ± 0.14
Phosphatidylethanolamines (PEs)	30.4 ± 0.6
Phosphatidylglycerols (PGs)	5.08 ± 0.42

Phosphatidylinositols (PIs)	5.32 ± 0.11
Phosphatidylcholines (PCs)	52.9 ± 0.5
Sphingomyelins (SMs)	2.68 ± 0.18

* Results are the means of three independent analyses (n=3) ± standard deviation (SD) values.
Abbreviation: PL – phospholipid.

3.1.2. FA composition in PC and PE fractions

For a deeper structural analysis of hen egg yolk PLs, the FA composition in the two main PL classes (PCs and PEs), representing over 80 % of total PLs, was determined. For this purpose, the PC and PE classes were separated and isolated by means of preparative TLC, derivatized to FAMEs, and then the FA compositions in each class were determined using GC-FID technique. The results showed statistically significant differences in FA composition between the two analyzed fractions. Saturated FAs (SFAs) accounted for approximately 48 % and 53 % of total FA peak areas in the PC and PE classes, respectively (Table 2). The most abundant FAs in PC species were palmitic acid (16:0) and stearic acid (18:0), whose amounts were 30.3 % and 17.2 % of total FAs, respectively. In contrast, PE fraction was characterised by higher content of stearic acid and lower of palmitic acid. Additionally, in both fractions, myristic (14:0), arachidic (20:0) and behenic (22:0) acids were identified, however, their concentrations were below 1 % of total FAs identified in hen egg yolk PLs.

Among the UFAs, in both PC and PE fractions, oleic acid (18:1; n-9) was the most abundant (Table 2). Another notable UFA present in both fractions at significant level was linoleic acid (18:2; n-6), whose concentrations were around 17.4 % and 11.7 % of total FAs, respectively for PC and PE species. Substantial difference between the two fractions was observed for arachidonic (20:4; n-6), and docosahexaenoic acid (22:6; n-3), both of which were more abundant in PE species. In addition, in the structures of both classes, palmitoleic (16:1) and α-linolenic (18:3) were found.

Table 2. Composition of FAs build-in the structure of PC and PE species.

FA	FA abbreviation	PC fraction	PE fraction
Saturated fatty acids (SFAs) [% of total peak areas]*			
Myristic	14:0	0.14 ± 0.02 [a]	0.41 ± 0.03 [b]
Palmitic	16:0	30.3 ± 0.3 [a]	18.4 ± 0.8 [b]
Stearic	18:0	17.2 ± 1.8 [a]	33.6 ± 2.2 [b]
Arachidic	20:0	0.14 ± 0.01 [a]	0.28 ± 0.01 [b]
Behenic	22:0	0.21 ± 0.01 [a]	0.56 ± 0.03 [b]
Total SFAs		**48.0 ± 1.5** [a]	**53.2 ± 1.5** [b]
Unsaturated fatty acids (UFAs) [%of total peak areas]*			
Palmitoleic	16:1 (n-7)	0.63 ± 0.01 [a]	0.19 ± 0.01 [b]

Oleic	18:1 (n-9)	27.6 ± 0.3 [a]	18.4 ± 0.8 [b]
Linoleic	18:2 (n-6)	17.4 ± 1.7 [a]	11.7 ± 0.3 [b]
α-Linolenic	18:3 (n-3)	0.12 ± 0.02 [a]	0.11 ± 0.01 [a]
Arachidonic	20:4 (n-6)	4.1 ± 0.7 [a]	12.0 ± 0.6 [b]
Docosahexaenoic	22:6 (n-3)	1.7 ± 0.4 [a]	3.9 ± 0.2 [b]
Total UFAs		**51.6 ± 1.8** [a]	**46.4 ± 1.5** [b]

* Results are the average of three independent analyses (n=3) ± standard deviation (SD) values. Different letters indicate significantly different values examined using unpaired Student's test ($p \leq 0.05$).

Abbreviations: FA – fatty acid; PC – phosphatidylcholine; PE – phosphatidylethanolamine; SFA – saturated fatty acid; UFA – unsaturated fatty acid.

3.1.3. Oxidation level of PL fractions

Hen egg yolk PLs were oxidized enzymatically in the presence of sodium deoxycholate using soybean LOX-1. Then, PL oxidation level was estimated using PV and TBARS assays. The first one provides quantitative information on the content of primary lipid oxidation products – lipid hydroperoxides. The other allows to monitor decomposition of lipid peroxidation products. As a result of lipid hydroperoxides decomposition by the C-C bond cleavage, truncated lipids and low-molecular weight volatile aldehydes such as 4-hydroxyhexanal (4-HHE), 4-hydroxynonenal (4-HNE) or MDA are formed. In acidic environment and increased temperature, MDA reacts with thiobarbituric acid (TBA) leading to the formation of MDA-TBA_2 adduct that can be quantified. Unfortunately, some other fatty peroxide-derived breakdown products may also react with TBA, giving rise increased result due to false TBA-positive substances (Catalán, Frühbeck, & Gómez-Ambrosi, 2018). The mentioned-above methods were employed for the characterization of PL fraction, both before and after LOX-catalyzed PL oxidation.

The enzymatic oxidation catalyzed by LOX is known to cause oxidative modification of UFAs. Accordingly, PV determined for FAs present in the structures of hen egg yolk PLs was statistically significantly higher ($p \leq 0.0001$) compared to native PL fraction (Table 3). In general, PV of fresh lipid fraction (e.g., edible oils) should be below 10 *mEq* O_2/kg (Gilbraith, Carter, Adams, Booksh, & Ottaway, 2021), while this parameter determined for oxidized PL fraction exceeded around 30 times the permissible level. This value measured for native fraction indicated that PLs were only slightly modified. The level of TBARS in non-oxidized sample was 0.22 mg/kg, also confirming high quality of the obtained PL fraction. In contrast, the amount of TBARS determined in oxidized PL sample was around 70 times higher ($p \leq 0.0001$) compared to the native PL fraction.

Table 3. Peroxide values and TBARS contents in native and oxidized PL fractions.

Parameters	Native PL fraction	Oxidized PL fraction
Peroxide value [*mEq* O_2/kg]*	1.3 ± 0.2 [a]	323 ± 22 [b]
TBARS [mg/kg]*	0.22 ± 0.04 [a]	15.3 ± 1.2 [b]

* Results are the means of three independent analyses (n=3) ± standard deviation (SD) values. Different letters indicate significantly different values examined using unpaired Student's test ($p \leq 0.05$).

Abbreviations: PL – phospholipid; TBARS – thiobarbituric acid reactive substances.

3.2. Characterization of aggregation structures containing native and oxidized PL

In aqueous environment PLs can form aggregation structures with different sizes, such as liposomes, mixed micelles and vesicles or lipid droplets. Because lipid digestion occurs at the oil/water interface, an important factor affecting the kinetics of lipid hydrolysis is the ratio between the surface area of aggregation structures and their volume. Therefore, it is important to characterize the hydrodynamic diameters of obtained aggregation structures before the enzymatic hydrolysis. For this purpose, non-invasive black scatter (NIBS) technique was employed. Its application enabled the determination of aggregation structure size distribution based both on the volume and number of analyzed objects. Additionally, the obtained population was characterized by polydispersity index (PDI) that assess the heterogeneity of the objects based on their size.

As a result of ultrasound treatment of PLs dissolved in SIF containing 5 mM BS, a homogeneous population of aggregation structures with an average diameter of 93 nm was obtained (Fig. A1A, Table 4). The particles were characterized by a slightly smaller diameter of 67 nm when this parameter was determined based on their number (Table 4). The PDI value of 0.15 confirmed the high homogeneity of the native PL sample.

Also for oxidized PLs, using as a basis the object number, the presence of a homogeneous aggregation structure population with an average diameter of 77 nm was found (Table 4). However, different size distribution was observed when the particle diameter was determined by volume (Fig. A1B). In this case, apart from the main object population with diameter of 122 nm, a second population was found with a diameter of 2.8 μm. The latter population accounted for over 35 % aggregation structures analyzed by volume. For this sample, the PDI value was 0.39 that suggest a significantly higher heterogeneity.

Furthermore, based on the obtained results, it can be stated that the presence of olive oil TAGs in aggregation structures containing both native and oxidized PLs influenced their size distribution. Using

the described earlier conditions, the population with hydrodynamic diameter around 56 nm was found for structures containing native PL fraction. Additionally, based on the object number, small population (~ 1 %) of aggregation structures with a size approximately 272 nm was observed (Table 4). A significantly different situation was observed in the size distribution determined by the object volume (Fig. A1C), where the population with a similar hydrodynamic diameter (~ 66 nm) represented only 33 %. The main population consisted of aggregation structures with a diameter of approximately 408 nm and accounted for 55 % of the total. Moreover, in the analyzed system, a small population with hydrodynamic diameter of 5,6 μm was detected. The PDI value for the native PL/BS/TAG emulsion was 0.50, which showed the significant influence of TAGs on the increase of heterogeneity of the sample compared to native PL/BS mixed micelle solution (PDI 0.15).

Also, the average diameter distribution (based on the object number) of aggregation structures composed of oxidized PLs, BSs and TAGs showed the presence of two populations, the main one with size of 63 nm and a smaller population (< 1 %) with hydrodynamic dimension of 405 nm (Table 4). Similarly to the previous sample type (native PL/BS/TAG emulsion), the size distribution measured based on the object volume was significantly different. The structural aggregations with average hydrodynamic dimension of 538 nm were predominant population. Additionally, two other populations of particles were observed: one with diameter of 76 nm and the other with 5.5 μm (Fig. A1D).

Table 4. PDI values and hydrodynamic diameters of aggregation structures PL/BS or PL/BS/TAG systems containing native or oxidized PLs.

System components	PDI*	The size of aggregation structures determined on the basis of			
		Object volumes		Object number	
		Diameter [nm]*	Content [%]*	Diameter [nm]*	Content [%]*
Native PLs + BSs	0.15 ± 0.02	93.0 ± 12.4	100	66.8 ± 1.9	100
Oxidized PLs + BSs	0.39 ± 0.03	122 ± 15	63.2 ± 15.7	77.0 ± 5.9	100
		2784 ± 693	36.8 ± 9.3	-	-
Native PLs + BSs + TAGs	0.50 ± 0.08	408 ±118	55.3 ± 4.7	55.9 ± 9.3	99.6 ± 0.5
		66.0 ± 14.0	33.3 ± 8.6	272 ± 23	0.78 ± 0.29
		5579 ± 216	4.0 ± 2.0	-	-
Oxidized PLs + BSs + TAGs	0.57 ± 0.09	538 ± 160	67.5 ± 6.9	62.6 ± 10.9	99.3 ± 0.2
		75.7 ± 25.0	31.6 ± 7.4	405 ± 82	0.69 ± 0.20
		5489 ± 99	2.6 ± 1.0	-	-

* Results are the means of five independent determinations (n=5) ± standard deviation (SD) values.

Abbreviations: BS – bile salt; PDI – polydispersity index; PL – phospholipid; TAG – triacyloglicerol.

3.3. PLA_2-catalysed hydrolysis of native and oxidized PLs embedded in mixed micelles and emulsions

Kinetics of PLA_2-catalysed hydrolysis of native and partially oxidized PLs present in mixed micelles or emulsions was determined using pH-stat method. This approach enabled monitoring of enzymatic hydrolysis of lipids based on the volume of NaOH solution used for neutralization of released FAs to maintain the pH at a constant value (pH=8 in this case) (Beisson, Tiss, Rivière, & Verger, 2000). Among all tested sample types, the native PL/BS mixed micelles were the most liable to hydrolysis catalyzed by PLA_2. After 10 min from the initiation of hydrolysis by the addition of PLA_2, approximately 26.4 mol % of FAs present in *sn*-2 position of PLs were released. In this period, the reaction proceeded at the highest rate (Fig. 2). The amounts of FAs released after 30 and 60 min were respectively 43.4 and 54.7 mol %, which clearly showed that the hydrolysis rate decreased with the reaction time. The addition of olive oil TAGs led to slight decrease of PL hydrolysis catalyzed by PLA_2. However, the differences in hydrolysis rate between native PL-containing systems without and with TAGs were not statically significant over the entire hydrolysis time range.

Oxidation of UFAs found in the structure of PLs caused a statistically significant slowdown of hydrolysis of oxPL/BS mixed micelles catalyzed by PLA_2. The discrepancy between hydrolysis rate of native and oxidized PL was growing especially in the range of 2 – 20 min. The amount of FAs released after 10 min of the reaction amounted to 20.2 mol % of FAs present in the *sn*-2 position of oxPLs, while this parameter achieved the value of 33.2 and 43.1 mol % after 30 and 60 min, respectively. For the oxPL/BS/TAG emulsion sample, the lowest digestibility by PLA_2 was observed. Similarly to the emulsion containing native PLs, the addition of olive oil TAGs slightly decreased the PL hydrolysis rate in oxPL/BS/TAG system, compared to mixed micelles with oxidized PL fraction. However, in these cases, the effect of TAG addition made statistically significant difference ($p \leq 0.05$) beginning from 40 min of the reaction. After 10 min of the hydrolysis, approximately of 18.6 mol % of FAs were released. Longer hydrolysis times (30 and 60 min) resulted in 30.2 and 39.0 mol % of FAs released from the *sn*-2 position of PLs, respectively.

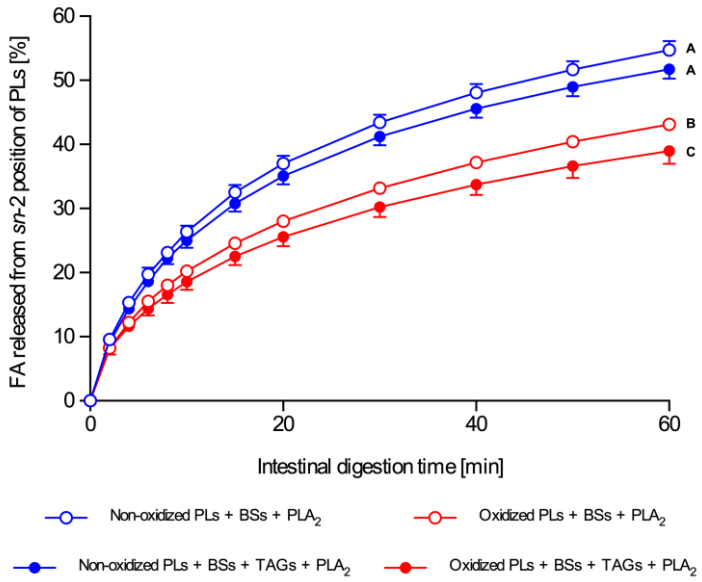

Fig. 2. PLA_2-catalysed hydrolysis of native and oxidized PL in the aggregation structures of mixed micelles and emulsions. The results are the average of three independent analyses (n=3). For the sake of legibility of the drawing, the standard deviation (SD) values in the graph is presented in one direction only (plus or minus). In the curve for oxidized PLs + BSs + PLA_2, the SD values were smaller than the symbol size used. Different letters at the endpoint of hydrolysis time indicate significantly different values examined using one-way ANOVA with Tukey's post hoc test ($p \leq 0.05$). (Abbreviations: BS – bile salt; FA – fatty acid; PL – phospholipid; PLA_2 – phospholipase A_2; TAG – triacyloglicerol)

3.4. Impact of hexanal and (*E*)-2-nonenal on PLA_2 activity

As mentioned earlier, low-molecular weight volatile aldehydes are formed as a result of degradation of lipid hydroperoxides by the cleavage of the C-C bond in UFA chains. Due to the frequent occurrence of linoleic acid in the structure of hen egg yolk PLs and its relatively high oxidability, hexanal was found to be one of the most abundant aldehydes among the volatile compounds identified in the headspace of the hen egg yolk PL fraction heated for 20 min at 100 °C (Chen, Balagiannis, & Parker, 2019). Another type of volatile aldehydes that are formed during lipid oxidation are electrophilic α-β-unsaturated aldehydes, which are susceptible to nucleophilic attack at the β-carbon position. The most abundant α-β-unsaturated aldehydes identified in the hen egg yolk PL fraction exposed to elevated temperature were (*E*)-2-heptenal, (*E*)-2-octenal, (*E*)-2-decenal and (*E*)-2-nonenal (Chen et al., 2019). In order to determine the effect of low-molecular volatile aldehydes on PLA_2 activity, two of those

aldehydes were used: hexanal and (*E*)-2-nonenal. The IC_{10} and IC_{30} values for both studied aldehydes are shown in Table 5.

The obtained IC_{10} and IC_{30} values were lower for (*E*)-2-nonenal compared to the saturated aldehyde – hexanal (Table 5). Importantly, in the case of both tested aldehydes – hexanal and (*E*)-2-nonenal– further increase in concentrations (above ~ 20 mM) did not lead to a linear decrease in the PLA_2 activity. Therefore, a 50 % reduction in enzyme activity was not achieved and consequently the IC_{50} values for neither of these aldehydes could be determined.

Table 5. Inhibitory concentration (IC) values determined for studied aldehydes causing 10 % and 30 % inhibition of porcine pancreatic PLA_2 activity.

Aldehyde	IC_{10} [mM]*	IC_{30} [mM]*
Hexanal	5.2 ± 0.6	15.7 ± 1.8
(*E*)-2-nonenal	3.3 ± 0.4	13.3 ± 1.5

* Results are calculated based on the equation of aldehyde concentration vs. percentage of PLA_2 inhibition in the linear range. All concentration points (0, 5, 10, 15, 20 mM) were determined in triplicate (n=3) ± standard deviation (SD) values for each aldehyde.

Abbreviation: PLA_2 – phospholipase A_2.

3.5. Impact on cell viability

The impact of native and oxidized PLs on HT29 cell viability was assessed using MTT test. The HT29 cell line was chosen as a model of the intestinal epithelium tissue that comes into direct contact with ingested food components. This cell line is recommended for nutritional studies i.a. by the National Centre for the Replacement, Refinement and Reduction of Animals in Research (UK) (Krishna & Gopalakrishnan, 2016) and a detailed explanation of the reason for choosing this cell line is presented in the section 1. Since earlier studies indicated that part of food-delivered PLs could be absorbed by intestinal cells without their prior hydrolysis (Zierenberg & Grundy, 1982), the cells were exposed to native and oxidized PLs in the presence of BS, both before and after intestinal hydrolysis. In the present study, two types of control cell cultures were used. The first one involved HT29 cells treated with the buffer (150 mM NaCl, 6 mM $CaCl_2$, 0.28 mM Tris-base, pH=8). The second type of control constituted of HT29 cells exposed to SIF that contained BS mixture at the concentration of 500 µg/mL. BSs are important surface-active compounds responsible for solubilization of food-delivered lipids, which enables their effective hydrolysis. Therefore, they are essential components of SIF used during *in vitro* intestinal digestion studies. In our study, BS mixture was used during lipolysis on native and oxidized PL fractions at the concentration of 5 mg/mL. However, the final concentration of BS mixture

in culture medium containing native or oxidized PLs before or after intestinal hydrolysis was 500 µg/mL. Additionally, the culture medium contained 0.5 µM Varespladib, which inhibits the PLA_2-catalyzed hydrolysis of PLs. The inhibitor was added to all types of cell cultures, including controls and cells exposed to non-hydrolyzed PLs, to eliminate its influence on cell viability while comparing treatments with different samples. The preliminary studies showed that Varespladib was not cytotoxic at the concentration used. Dose-response curves after 6, 24, 48 and 72 h of cell exposure to native and oxidized PLs before and after hydrolysis are shown in **Fig. 3**. Results of the statistical analysis are available in the Supplementary Materials (Table A3).

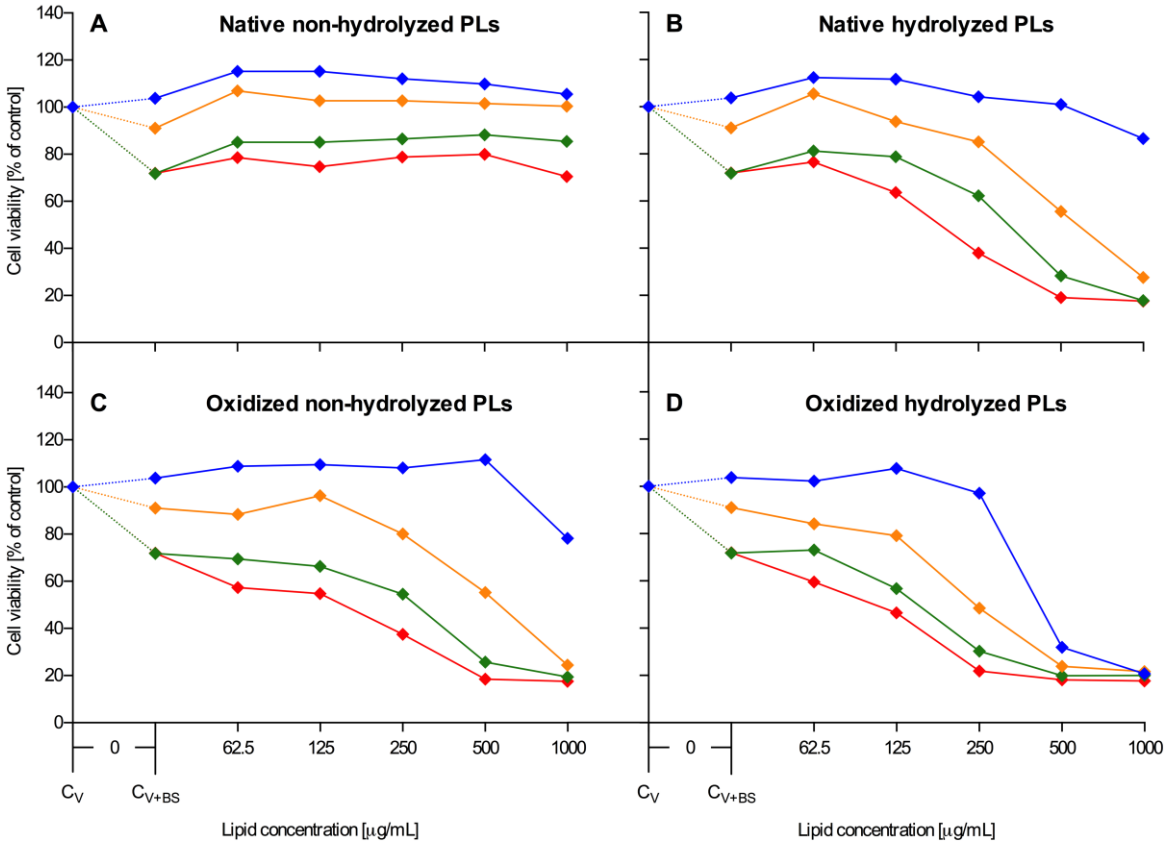

Fig. 3. Cell viability of HT29 cells determined by MTT test after 6 (blue), 24 (orange), 48 (green) and 72 h (red) exposure to: native non-hydrolyzed PL/BS mixed micelle solution (A); native hydrolyzed PL/BS mixed micelle solution (B); oxidized non-hydrolyzed PL/BS mixed micelle solution (C) and oxidized hydrolyzed PL/BS mixed micelle solution (D). Results represent means of three independent experiments carried out in quadruplicate (standard deviation (SD) values are lower than 15 %). Results of statistical analysis are available in Supplementary Materials (Table A3). (Abbreviations: BS – bile salt; C_v – control cells treated with buffer containing 0.5 µM Varespladib; C_{v+BS} – control cells

706 treated with SIF containing 500 µg/mL BSs and 0.5 µM Varespladib; PL – phospholipid; SIF –
707 simulated intestinal fluid)
708 The exposure of HT29 cells to SIF containing only a BS mixture led to the decrease of their viability
709 (Fig. 3). This effect was observed especially for prolonged treatment times (48 and 72 h), for which the
710 decrease of cell viability was around 30 %, while for 24 h the cell viability achieved around 90 %
711 compared to control cells exposed to buffer only. Importantly, the simultaneous presence of native
712 non-hydrolyzed PLs, across the range of concentrations used (62.5 – 1000 µg/mL), led to a reversal of
713 the cytotoxic effect of BS for all tested exposure times (Fig. 3A). Additionally, there was no significant
714 effect of the increasing PL concentration on cell viability. However, it was observed that the prolonged
715 exposure times (48 and 72 h) decreased the viability of the cells compared to the control ones treated
716 with buffer only..
717 PL digestion catalyzed by PLA_2 leads to the formation of 1-LPL and FA. In our experiments, after
718 releasing 40 % of the FAs present at the *sn*-2 position of PL, the reaction was terminated by the
719 addition of PLA_2 inhibitor Varespladib. For this sample type, containing native PL and product of their
720 lipolysis, the reduction of the cytotoxic effect of BS was observed in the case of the lowest lipid
721 concentration used (62.5 µg/mL) for all tested exposure times (Fig. 3B). However, the protective effect
722 was not observed for higher concentrations (125 – 1000 µg/mL). For the shortest incubation time (6 h),
723 only the highest concentration tested (1000 µg/mL) caused a decrease in cell viability by about 15 %
724 compared to the buffer-treated control cells. While, for exposure times of 24, 48 and 72 h, there was a
725 significant dose-dependent decrease in HT29 cell viability with an increase in the concentrations of
726 PLs and products of their hydrolysis (1-LPL and FA) in the tested mixtures containing constant BS
727 concentration.
728 The oxidative modification of PL significantly contributed to the viability of HT29 cells compared to
729 their native counterparts (Fig. 3C). In the case of the shortest incubation time (6h), no significant
730 decline in HT29 cell viability was observed in the concentration range of 62.5 – 500 µg/mL. However,
731 the cell exposure to the highest concentration of oxidized PL at the same incubation time (6 h) led to a
732 20 % decrease of cell viability. For longer exposure times in the range of 24 – 72 h, negative
733 correlation between oxidized PL concentrations and cell viability was observed. A significant decrease
734 in cell viability , for these treatment times, was observed for all concentrations above 125 µg/mL.

735 Furthermore, for this sample type, no significant protective effect against BS-induced cytotoxicity was
736 observed.
737 The oxidized PLs after their partial hydrolysis (around 40 % of total PL) were characterized by the
738 highest cytotoxicity among all tested samples (Fig. 3D). For the incubation time of 6 h, no significant
739 decrease in HT29 cell viability was observed in the concentration range of 62.5 – 250 μg/mL. Above
740 this range, a sharp decrease in cell survival was observed, reaching around 70 % decline in cell
741 viability for concentration of 500 μg/mL. For the incubation times of 24, 48 and 72 h, negative
742 correlation between lipid (PL/1-LPL/FA) concentrations and cell viability was observed. For 24 and 48
743 h exposure times, maximum reduction of cell viability was observed for concentrations of 500 and
744 1000 μg/mL, while for 72 h the maximum viability decrease was achieved for consternations above
745 250 μg/mL. Similarly to oxidized non-hydrolyzed PLs, the protective effect against cytotoxicity induced
746 by BS mixture was not observed for oxidized PL fraction after partial hydrolysis.
747 **3.6. Genotoxicity**
748 The effect of native and oxidized PL before and after hydrolysis on the DNA integrity of cells treated
749 for 24 h with tested samples was determined by a comet assay. The test is based on the detection of
750 DNA strand breaks in single cells embedded in LMP agarose (single-cell gel electrophoresis test). The
751 lipid concentrations used in the comet assay (125 and 250 μg/mL) were selected on the basis of the
752 results obtained by MTT test, so that the viability of HT29 cells treated for 24 h with the tested
753 solutions was not lower than 80 % of control cell viability. The only exception was the cells exposed to
754 oxidized PL/BS mixed micelles after partial hydrolysis, where the cell viability was inhibited by about
755 50 % for the concentrations of 250 μg/mL.
756 Among all tested samples, the treatment with BS mixture alone at the concentration of 500 μg/mL
757 caused the highest genotoxicity (Fig. 4). Interestingly, the BS-induced the genotoxic effect was similar
758 to DNA damage observed in the case of positive control cells treated with 150 μM H_2O_2 for 1 h. The
759 percentage of DNA in tail for these samples was 21.2 and 26.5 %, respectively. On the other hand, the
760 obtained results indicated that the simultaneous presence of PLs, either native or oxidized before and
761 after hydrolysis at both tested concentrations (125 and 250 μg/mL), significantly reduced BS-induced
762 DNA fragmentation. Moreover, for most of the tested sample types, a statistically significant difference
763 in DNA integrity was observed between the two applied concentrations, with 250 μg/mL offering better
764 protection. The statistical analysis does not confirm concentration dependence only for native non-

765 hydrolyzed PL, for which the p value was 0.1148. Overall, however, the same effect on BS-induced
766 genotoxicity was observed regardless of PL oxidation or hydrolysis.

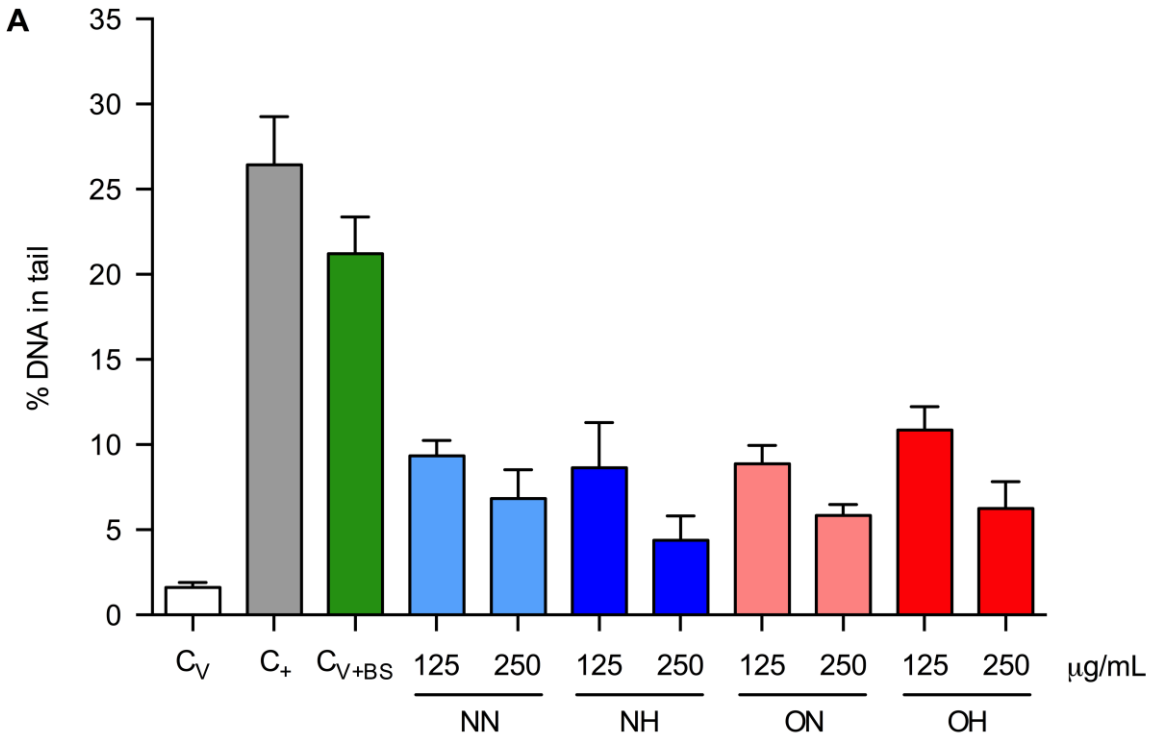

B

vs.	C_+	C_{V+BS}	NN 125	NN 250	NH 125	NH 250	ON 125	ON 250	OH 125	OH 250
C_V	**<0.0001**	**<0.0001**	**<0.0001**	**0.0001**	**<0.0001**	0.0577	**<0.0001**	**0.0010**	**<0.0001**	**0.0002**
C_+		**<0.0001**	**<0.0001**	**<0.0001**	**<0.0001**	**0.0195**	**<0.0001**	**<0.0001**	**<0.0001**	**<0.0001**
C_{V+BS}			**<0.0001**	**<0.0001**	**<0.0001**	**<0.0001**	**< 0.0001**	**<0.0001**	**<0.0001**	**< 0.0001**
NN 125				0.1148	0.9987	**<0.0001**	>0.9999	**0.0040**	0.7845	**0.0183**
NN 250					0.5527	0.1471	0.3725	0.9861	**0.0004**	0.9998
NH 125						**0.0002**	>0.9999	0.0541	0.2484	0.1722
NH 250							**<0.0001**	0.8107	**<0.0001**	0.5039
ON 125								**0.0251**	0.4020	0.0912
ON 250									**<0.0001**	>0.9999
OH 125										**<0.0001**

767

768 **Fig. 4.** Genotoxic effects of native and oxidized PL/BS mixed micelles before and after hydrolysis
769 determined in HT29 cells by comet assay and expressed as % DNA in the comet tail (Panel A).
770 Results represent means of three independent experiments and standard deviation (SD) values. In the
771 graph, the SD values are presented only in the plus direction. The final concentration of PLA_2 inhibitor
772 in cell medium for all tested samples was 0.5 µM. Probability values for individual sample pairs were
773 compared using one-way ANOVA with Tukey's post hoc test. Values with statistically important
774 difference ($p < 0.05$) between the two compared samples are marked in bold red, while probability
775 values $p \geq 0.05$ in normal font (panel B). (Abbreviations: BS – bile salt; C_+ – positive control cells

776 treated with 150 μM H_2O_2 for 1 h; C_v – control cells treated with buffer containing 0.5 μM Varespladib;
777 C_{v+BS} – control cells treated with SIF containing 500 μg/mL BSs and 0.5 μM Varespladib; NH – native
778 hydrolyzed; NN – native non-hydrolyzed; OH – oxidized hydrolyzed; ON – oxidized non-hydrolyzed;
779 PL – phospholipid; PLA_2 – phospholipase A_2; SIF – simulated intestinal fluid)

780 **3.7. Neutral lipid accumulation**

781 CLDs are intracellular organelles composed of a core containing neutral lipids (mainly TAGs)
782 surrounded by a PL monolayer with various proteins embedded in it. CLDs can be visualized using
783 fluorescence microscopy after staining of CLDs with lipophilic dye – Nile Red. In a neutral lipid
784 environment (e.g., CLD core), Nile Red exhibits green fluorescence with a maximum emission at the
785 wavelength of 585 nm (excitation wavelength of 510 nm). In contrast, in PL-rich structures (e.g.,
786 cellular membranes), Nile Red exhibits red fluorescence with emission and excitation wavelengths of
787 640 and 550 nm, respectively. In the present study, the accumulation of natural lipids in CLDs was
788 assessed using the green fluorescence of Nile Red (Listenberger & Brown, 2007). Before CLD
789 imagining, HT29 cells were treated for 24 h with native or oxidized PL/BS mixed micelles (125 μg/mL)
790 before and after hydrolysis catalyzed by PLA_2.
791 Visual analysis of the fluorescence intensity of CLDs present in HT29 cells suggested that the
792 presence of free FA increases the accumulation of neutral lipids since it was significantly higher for
793 native and oxidized PL/1-LPL/FA mixture compared to non-hydrolyzed PLs (Fig. 5). There was
794 however no effect of PL oxidation on fluorescence intensity, which indicates no increase in the
795 accumulation of neutral lipids. No differences were observed, between cells exposed to non-
796 hydrolyzed both native or oxidized PLs and control cells treated with the buffer (150 mM NaCl, 5 mM
797 $CaCl_2$, 0.28 mM Tris) containing 5 μM Varespladib. Additionally, based on the visual analysis, there
798 was no influence of BS mixture (500 μg/mL) on lipid accumulation.

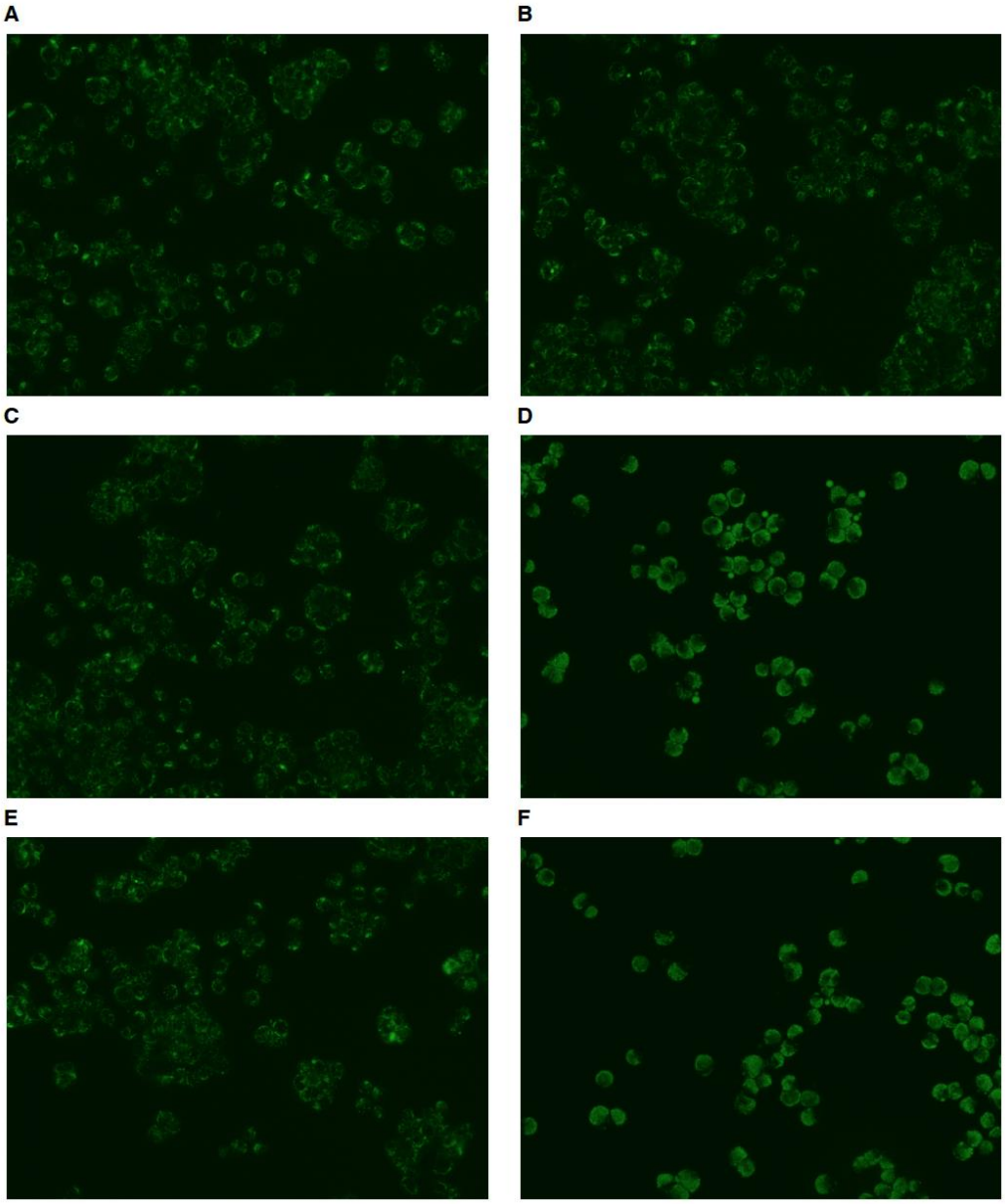

Fig. 5. Visualization of CLDs in HT29 cells after 24 h exposure to PL/BS mixed micelles intact or submitted to PLA_2 catalyzed hydrolysis using fluorescent microscopy and Nile Red staining: cells treated with buffer containing 0.5 μM Varespladib (A); cells treated with SIF containing 500 μg/mL BSs and 0.5 μM Varespladib (B); cells treated with native PL/BS mixed micelle solution (C); cells treated with native PL/BS mixed micelle solution after hydrolysis (D); cells treated with oxidized PL/BS mixed micelle solution (E) and cells treated with oxidized PL/BS mixed micelle solution after hydrolysis (F). The final concentrations of PL and BS in cell medium containing mixed micelles were 125 and 500 μg/mL, respectively. (Abbreviations: BS – bile salt; CLD – cytosolic lipid droplet; PL – phospholipid; PLA_2 – phospholipase A_2)

4. Discussion

Oxidative modifications of FAs found in the structure of lipids lead to the loss of the nutritional value and deterioration of sensory properties of food products (Jacobsen, Paiva-Martins, Schwarz, & Bochkov, 2019). Moreover, a variety of harmful substances can be formed, including lipid hydroperoxides and products of their decomposition, containing hydroxy, epoxy, keto or aldehyde groups. It has been estimated that daily intake of LOOHs is around 1.5 mmol (Kanner, 2007). While the consumption of acrolein (α-β unsaturated aldehyde formed from PUFAs *via* LOOHs) can significantly exceed 1 mg per day (according to some data the maximum exposure is 0.1 mg/kg/day (Henning, Johnson, Coyle, & Harbison, 2017; Vieira, Zhang, & Decker, 2017)), which is far above the Tolerable Daily Intake (TDI) value of 7.5 µg/kg/day recommended by the World Health Organization (WHO) (Jiang et al., 2022). Unfortunately, general health recommendations for the maximum acceptable human daily intakes (MHDIs) of other LOPs are either extremely limited or completely unavailable (Grootveld, Percival, Leenders, & Wilson, 2020).

An *in vivo* study in a rat model fed with non-oxidized and oxidized (PVs in the range of 100 – 1200 *mEq* O_2/kg) soybean oils indicated that animal exposure to oils with PVs above 400 *mEq* O_2/kg significantly decreased weight gain compared to the control group. A diet containing oxidized oil with a PV of 1200 *mEq* O_2/kg caused deaths within the approximately three weeks. Among the symptoms, weight loss during the experiment and severe diarrhea were observed. Animals fed with oil characterized by PV of 800 *mEq* O_2/kg developed moderate to severe diarrhea, but the symptom had subsided somewhat by the eighth week. Additionally, the histological examinations of the animals fed with highly oxidized fraction (PV above 3000 *mEq* O_2/kg) indicates that intestines were one of the most affected organs and were characterized by the presence of cytoplasmic vacuoles distending mucosal (Andrews, Griffith, Mead, & Stein, 1960). Cases of food poisoning manifested by acute symptoms such as diarrheal, nausea, emesis, abdominal pain, fatigue, and headache, were also observed in humans consuming processed foods containing oils and fats with PVs of at least 100 *mEq* O_2/kg (Gotoh et al., 2006). Moreover, chronic consumption of such foodstuffs has been postulated to increase the risk of disorders such as alimentary tract cancers, cardiovascular diseases and nervous system disorders (neurotoxicity) (Gotoh et al., 2006; Jackson & Penumetcha, 2019). Therefore, it seems important to understand the influence of oxidation of dietary lipid on important physiological processes occurring in the intestinal lumen, namely digestion and up-take as well as the subsequent biological effects of lipid oxidation and hydrolysis towards IECs.

To address these questions, in the present study, we used PL fraction isolated from hen egg yolk that is the main nutritional source of PLs in typical Western diet (Blesso, 2015). As shown in Table 2, hen egg yolk PL species contained a significant share of UFAs, including PUFAs such as α-linolenic or arachidonic acids. Therefore, PL fraction isolated from egg yolk was selected as a suitable model for oxidation and further assessment of its impact on IECs. In general, oxidized lipids can be formed in three ways: by non-enzymatic autoxidation and photo-oxidation or *via* enzyme-catalysed reaction, but all of these reactions lead to the formation of lipid hydroperoxides as primary oxidation products (Domínguez et al., 2019). However, to ensure a high yield of PL oxidation needed in our study, the LOX-catalysed reaction was chosen. The PV determined for oxidized PL fraction (323 *mEq* O_2/kg) confirmed that PL species were oxidized with high efficiency and could be successfully used in further stages of our research (Table 3). Our previous analysis, using two-step high-performance liquid chromatography (HPLC) coupled with mass spectrometry (MS) technique, confirmed the presence of not only PL hydroperoxides, but also PL dihydroperoxides in the LOX-catalysed hen egg PL fraction (Parchem, Kusznierewicz, et al., 2019). The latter are not typical lipid oxidation products, however, previous studies indicated that they can be formed *in vitro* at high enzyme concentration (Brash, 1999). Additionally, lipid dihydroperoxides were detected in virgin and refined soybean oils exposed to elevated temperature (70°C) (Martin-Rubio, Sopelana, Ibargoitia, & Guillén, 2021). Our current study also showed a statistically significant difference in TBARS content between oxidized and native fraction (Table 3). This indicated at least a partial decomposition of full-chain length PL (di)hydroperoxides by C-C bond cleavage and formation of low-molecular weight aldehydes, known to inhibit pancreatic PLA_2 activity, and thereby obstructing PLs hydrolysis (Litvinko et al., 2018).

In the next step of the study, the effect of PL oxidation on the parameters of aggregation structures present in SIF containing BS mixture was evaluated. In general, PLs can form different aggregation structures, whose spatial organization depends on the presence and composition of surfactants (e.g., BSs), other lipid molecules (e.g., TAGs), non-lipid compounds (e.g., proteins) as well as on physicochemical properties of aqueous phase (Birru et al., 2014; Meyuhas et al., 1997). Under the conditions used in our study, native PLs formed the homogeneous population of aggregation structures. Taking into account their size (67 and 93 nm based on the object number and volume, respectively), it can be assumed that the PL/BS mixed micelles or/and vesicles were obtained. The typical size of mixed micelles, based on the literature data, ranges from 50 to 150 nm (Riethorst et al.,

2016), while this parameter for mixed vesicles achieves values from 50 to several hundred nm (Birru et al., 2014), though unequivocal identification of aggregation structure type is not possible only on the basis of their size. In this study, the obtained aggregation structures are referred to as mixed micelles, however, noted that unambiguous identification was not made in this study. The size distribution of native PL/BS sample (Fig. A1A) indicated also the presence of structures with the diameter below 50 nm, which are most likely single-component BS micelles. Their typical size ranges from 10 to 50 nm (Riethorst et al., 2016). The replacement of native PLs by their oxidized counterparts led to slightly increased hydrodynamic diameter of the structures formed (Table 4, Fig. A1B). This can result from the displacement of oxidized FAs present in surface PLs from hydrophobic part of the aggregation structure towards the aqueous environment, which is related to the increased hydrophilicity of FAs due to their oxidative modification. Consequently, the hydrophilic groups of oxidized FAs could interact with water molecules leading to the formation of solvation shell and increase in hydrodynamic diameter. The presence of oxidized FAs on the liposome surface has also been suggested in previous studies, in which a model composed of cholesterol and PC species with hydroperoxy linoleic acid was applied (Kambayashi, Yamamoto, & Nakan, 1998). Moreover, the size distribution of the oxidized PL/BS structures determined by volume revealed not only the major population with the hydrodynamic dimension of 122 nm, but also another fraction with a much larger dimension of 2.8 μm. This could be a result of the aggregation of the primary structures into larger clusters *via* e.g., cross-linking of PL molecules by imine formation. Such reaction is known to occur between the primary amines found in the PE head group (ethanolamine) and the aldehyde groups. The latter can be present in the structure of truncated oxPL formed by C-C bond cleavage along UFA acyl chain. Importantly, oxidation of PLs followed by imine formation was reported as a necessary step in sphingosine-induced vesicles aggregation (Jiménez-Rojo et al., 2014).

The addition of olive oil TAGs to native and oxidized PL/BS systems resulted in significant changes of the size distributions based on object volume compared to TAG-free systems (Fig. A1). For native PLs, a heterogeneous system was obtained with the main population characterised by hydrodynamic diameter of 408 nm. It may be postulated that lipid droplets were formed under the conditions used. Their typical size, according to literature data, ranges from 20 to 500 nm for lipid droplets forming nanoemulsion, while aggregation structures with dimension of 1 – 100 μm are typical for macroemulsions (A. Gupta, Eral, Hatton, & Doyle, 2016). Additionally, the lipid droplets with the size

specific for macroemulsions (5.6 μm) were also observed in our system. However, their share was small and accounted for about 4% based on particle volume. The second most abundant population in the analyzed system were aggregation structures with the size below 100 nm, which corresponds to small lipid droplets present in nanoemulsion (A. Gupta et al., 2016). Importantly, these structures represented a practically homogeneous population when the size distribution was based on the object number. Similarly to PL/BS models, the use of oxidized PLs had a slight effect on the size distribution of the structures composed of PLs, BSs and TAG compared to native ones. Most likely this was associated with changes in spatial structure and physicochemical properties of PL species containing oxidized FAs that affected their behaviour during the assembly of the aggregation structures. Although the addition of olive oil TAGs to the system containing native PLs and BS mixture affected the size distribution of formed aggregation structures, no effect was observed on the PL hydrolysis catalyzed by pancreatic PLA_2. This suggested that in both analyzed systems (without and with TAGs), the enzyme had an unimpeded access to the substrates located on the surface of aggregation structures. In contrast, a significant decrease in the hydrolysis rate was observed for the systems containing oxPLs, especially in the model containing additionally TAGs. As already mentioned, PL hydroperoxides are preferentially hydrolyzed by PLA_2 compared to the native counterparts, at least when standard PC hydroperoxide (PC18:0/18:2(-OOH)) was used (Baba et al., 1993). In contrast, another study suggested that UV-irradiation of hen egg yolk PL/sodium deoxycholate mixed micelles decreased porcine pancreatic PLA_2 activity after 40 min of the reaction. In this case, however, the authors linked their observation to significant increase of MDA level formed over this time (Litvinko et al., 2018). Therefore, in our study we have attempted to determine the effect of low-molecular aldehydes on the porcine pancreatic PLA_2 activity.

The chemical structures of formed aldehydes depend on the structure of precursor UFA (e.g., n-6 or n-3 family) and the oxidation pathway. In general, saturated and α-β-unsaturated aldehydes, can be distinguished. In our study, we determined the effect of hexanal and (*E*)-2-nonenal – representatives of saturated and unsaturated aldehydes, respectively, previously identified in the hen egg yolk PL fraction exposed to elevated temperature (Chen et al., 2019) – on PLA_2 activity. The obtained data indicated that both tested aldehydes showed the ability to inhibit this enzyme with (*E*)-2-nonenal being more effective inhibitor of PLA_2 activity (Table 5). Aldehydes can covalently modify enzymes by electrophilic addition to primary amines of the amino acids, such as lysine and arginine, with the

formation of Schiff's bases. Porcine pancreatic PLA_2 (1SFW according to the PDB database) is a small enzyme composed of 124 amino acids. Its active side includes His-48, Asp-99 and Ca^{2+} ion that is bound by Tyr-28, Gly-30, Gly-32, Asp-49. Additionally, PLA_2 structure is stabilized by seven disulfide bonds, which makes this enzyme highly resistant to chemically and thermally induced unfolding (Kölbel, Weininger, Ihling, Mrestani-Klaus, & Ulbrich-Hofmann, 2015). However, there are nine lysine and four arginine residues in the amino acid sequence of PLA_2 that may be modified by the mentioned aldehydes, which can cause the change in the enzyme conformation and lower its activity. As described earlier, for both tested aldehydes, the reduction of enzymatic activity by 50 % could be not achieved, despite the increases in aldehyde concentration. This explanation could be that after reaching a certain aldehyde concentration, all possible liable to modification enzyme sites become modified, leading to a decrease in its activity, but not complete inactivation. Therefore, an increase in the aldehyde concentration did not cause further reduction of enzymatic activity.

Summarizing this part of the work, it can be stated that oxidation of dietary (phospho)lipids, and consequently the formation of low-molecular weight aldehydes, declines (ox)PL digestibility by pancreatic PLA_2. Moreover, it seems that this enzyme is responsible not only for direct PL digestion, but also may modulate digestion of TAGs catalyzed by pancreatic lipase-colipase complex (Borgström, 1980). The role of PLA_2 in neutral lipid digestion is to facilitate the access of lipase to TAGs present in the core of lipid droplets surrounded by dietary and bile PLs. The initiation of PL hydrolysis by PLA_2 results in binding of lipase to their substrates and rapid hydrolysis of TAGs (Borgström, 1980). Taking the above into account, it can be hypothesized that PLA_2 activity decline in the presence of oxidized (phospho)lipids is a physiological protective mechanism against too rapid release of oxidized FAs, which similarly to their native counterparts may be effective absorbed by IECs (Penumetcha, Khan, & Parthasarathy, 2000). Otherwise, in the cells exposed to relatively high concentration of oxidized lipid hydrolysis products, the cellular redox homeostasis could become disturbed and IEC death induced (T. Wang, Gotoh, Jennings, & Rhoads, 2000).

In order to examine this hypothesis, we evaluated the biological effect of PL oxidation and hydrolysis towards HT29 cells serving as a model of IECs. However, it should be reminded the cell line used in this study is characterized by cancerous origin. Therefore, due to some changes in nutrient transport and metabolism as well as redox status, the tested compounds can affect the cells differentially compared to healthy intestinal cells. Nevertheless, the aim of our research was to understand the

general mechanism of toxicity of oxidized PLs and products and their hydrolysis in the presence of BSs, therefore we found this model to be appropriate. Based on the data obtained using MTT test, it was observed that hydrolysis and oxidation of PLs led to significant decrease of cell viability in a time- and concentration-dependent manner, while oxidized hydrolyzed PLs were characterized by the highest cytotoxic effect (Fig. 3, Table A3). Additionally, BSs alone were found to decline HT29 cell viability, especially for prolonged exposure time, compared to control cells treated with the buffer only. However, this effect was reversed by the simultaneous presence of native non-hydrolyzed PLs across the range of concentrations used. This observation can be explained by the limited bioavailability of BSs for cells due to promoting the formation of less cytotoxic PL/BS mixed micelles/vesicles, which was also confirmed by previous studies using other intestinal epithelium cell line delivered form human colorectal adenocarcinoma – Caco-2 (Tan et al., 2013). Most probably, such a protective effect also occurs under physiological conditions, where BSs are released to duodenum in the bile form containing PLs. Bile is composed of 95 % water and various inorganic and organic compounds. The letter include *i.a.* bile acids (40 mM), PLs (7 mM), cholesterol (3 mM) (Macierzanka, Torcello-Gómez, Jungnickel, & Maldonado-Valderrama, 2019).

In addition, comet assay results showed that cell exposure to BS mixture caused significant DNA strand breaks (Fig. 4). The genotoxic mechanism of BSs is not yet fully understood. It has been suggested that DNA damage can be caused by the increased production of ROS and RNS *via* stimulatory effect of BSs on the activation of LOX, cyclooxygenase (COX) and NADPH oxidase (Nguyen, Ung, Kim, & Jung, 2018; Rosignoli et al., 2008). Moreover, BSs due to their surfactant properties can cause mitochondrial damage, leading to the release of ROS generated in the mitochondrial electron transport chain (Nguyen et al., 2018). However, the BS-induced genotoxicity was reversed in the presence of not only native non-hydrolyzed PLs, as observed in the case of cytotoxic effect of BS, but also in cells treated with oxidized and hydrolysed samples. Moreover, higher lipid concentration (250 vs. 125 µg/mL) led to statistically significant stronger protection against BS-induced genotoxicity for all sample types. This observation indicates that cytotoxic effect caused by prolonged cell exposure to higher concentrations of native hydrolyzed and oxidized, both non-hydrolyzed and hydrolyzed PLs, was not related to DNA strand breaks, as determined using comet assay. Most probably, for HT29 cells treated with these samples, an overlap of other toxic effects was observed. For example, hydrolysis of both native and oxidized PLs significantly affected the cellular

accumulation of neutral lipids. The products of PL hydrolysis (LPLs and FAs), after intestinal absorption, are re-esterified at the ER membrane (Küllenberg de Gaudry et al., 2012). However, the prolonged cell exposure to high concentration of LPLs and FAs can lead to excessive of cellular PL levels causing alterations in cellular lipid metabolism. The previous data showed that cell exposure to exogenous LPCs or LPEs led to increased synthesis of cellular PCs. However, the cells compensated this elevated PC level by their enzymatic degradation to glycerophosphocholine (GPC) and FA by lysophospholipase (lysoPLA$_1$) activity (Baburina & Jackowski, 1999).

Additionally, taking into account the presence of FAs delivered from egg yolk PL hydrolysis in the culture medium, cellular esterification of these FAs to TAGs would be necessary to limit their lipotoxic effect (Lipke, Kubis-Kubiak, & Piwowar, 2022). This metabolic pathway most probably led to increased accumulation of TAGs in the cytosolic droplets within the cells exposed to hydrolyzed native and oxidized PLs. However, long-term cell exposure to high concentration of PL hydrolysis products could lead to the intensification of the lipotoxic effect, which was manifested as decreased cell viability. Importantly, under the lipotoxic conditions, the increased mitochondrial FA oxidation can occur in order to metabolize the cellular lipid excess. This can lead to disturbance of cellular redox homeostasis and increased lipid peroxidation accompanied by the formation of other toxic compounds such as electrophilic α,β-unsaturated 4-hydroxyalkenals, which are capable of covalent modification of cellular proteins or DNA. Such type of DNA damage however, may not be detected by comet assay used in this study. This method determines DNA strand fragmentation, but not necessarily the stable covalent modifications of nucleic acid bases by aldehydes.

HT29 cell exposure to non-hydrolyzed oxidized PLs led to a significant decrease of their viability, especially for prolonged incubation times. On the one hand, absorption of (phospho)lipid oxidation products containing reactive functional groups, such as hydroperoxide or aldehyde, can led to modification of cellular structures such as proteins, membrane lipids and DNA, as well as may disturb the cellular redox homeostasis. The previous research using other cell line – Caco-2 – confirmed our observations and conclusions. The exposure of Caco-2 cells to not-hydrolyzed oxidized menhaden oil lead to significant GSH/GSSG ratio, inducing cellular redox imbalance and initiation of apoptotic cell death (T. Wang et al., 2000). Moreover, the literature data indicated that oxPLs can trigger numerous signaling pathways leading also to cellular apoptosis as well as inflammation induction (Fruhwirth et al., 2007). Interestingly, the biggest differences in the cell viability curves were observed between

native hydrolyzed, oxidized non-hydrolyzed and oxidized hydrolyzed PLs for the cells exposed the shortest incubation time (6 h). This indicates that while comparing all, the release of oxidized FAs from the *sn*-2 position of PLs in a short time induced the highest cytotoxic effect among all tested samples. An *in vitro* studies using Caco-2 cell line indicated that hydroperoxy octadecadienoic acid (HPODE) and hydroxy octadecadienoic acid (HODE) were effectively absorbed by cells within the exposure time of 30 min. Additionally, the uptake of modified FAs was comparable to non-oxidized FAs such as linoleic or oleic (Penumetcha et al., 2000). In contrast, the absorption of these oxidized FAs was significantly (about 20 times) lower for smooth muscle cells (Penumetcha et al., 2000). One of the most common oxidized FA is 13-hydroperoxy octadecadienoic acid (13-HPODE). In addition to inducing oxidative stress and cellular death at higher concentrations (above 100 μM) and insufficient activity of GPx2 enzyme, an *in vitro* studies using Caco-2 model showed that subtoxic concentration of 13-HPODE can induce pro-inflammatory gene expression and affect lipid and glucose metabolism, energy production and mitochondrial functions (Faizo, Narasimhulu, Forsman, Yooseph, & Parthasarathy, 2021; Keewan, Narasimhulu, Rohr, Hamid, & Parthasarathy, 2020).

5. Conclusions

Oxidation of dietary (phospho)lipids is associated not only with the deterioration of the quality and sensory properties of foodstuffs, but also may pose a serious threat to the health of consumers, especially leading to some gastrointestinal pathologies. Firstly, our results indicated that oxidation of PLs decreased their hydrolysis catalyzed by pancreatic PLA_2 in the presence of BS mixture. We suggested that low-molecular weight aldehydes such as hexanal or (*E*)-2-nonenal, which are formed as a result of lipid hydroperoxide breakdown by the cleavage of the C-C bond in UFA chains, can covalently modify the enzyme leading to inhibition of its activity. Our further research using HT29 cell line indicated that both hydrolysis and oxidation of PLs led to decrease of cell viability in a time- and concentration-dependent manner, while combination of both these factors resulted in the highest cytotoxic effect determined by MTT test. On the other hand, the BS-induced genotoxic effect was reversed in the presence PLs regardless of whether they were oxidized or hydrolyzed, while the protective effect against the BS-induced cytotoxicity was observed for native non-hydrolyzed PLs, but was not clearly visible for other samples. This can be related to an overlap of several toxic effects including lipotoxicity or disturbance of cellular redox homeostasis. The obtained data have driven us to a non-obvious conclusion that the inhibition of PLA_2 activity in the presence of oxidized

(phospho)lipids, may be a kind of physiological protective mechanism against rapid release of oxidized FAs that are characterized by cytotoxic effect towards IECs.

6. Limitation of the study

It should be noted that the presented work was aimed at a preliminary assessment of the influence of oxidative modification of dietary (phospho)lipids on their digestion and biological effects towards intestinal epithelium. Therefore, to understand the fundamental mechanisms or their action, the proposed models did not fully reflect the physiological conditions (e.g., only the intestinal phase of digestion was considered; only one of pancreatic lipolytic enzymes was used; there were no other nutrients such as protein included). However, despite simplified experimental design, it was possible to observe the important differences between native and oxidized egg yolk PL fractions on PL hydrolysis as well as cell physiology and pathophysiology. Nevertheless, further work in this area is needed for a deeper understanding of mechanisms occurring under the physiological conditions.

CRediT authorship contribution statement

Karol Parchem: Conceptualization, Data Curation, Formal analysis, Funding Acquisition, Investigation, Methodology, Project Administration, Validation, Visualization, Writing – original draft, Writing – review & editing. **Monika Baranowska:** Investigation, Methodology, Validation. **Anna Kościelak:** Investigation. **Ilona Kłosowska-Chomiczewska:** Investigation, Methodology, Validation. **Maria Rosário Domingues:** Funding Acquisition, Supervision, Writing – review & editing. **Adam Macierzanka:** Supervision, Writing – review & editing. **Agnieszka Bartoszek:** Conceptualization, Formal analysis, Funding Acquisition, Resources, Supervision, Visualization, Writing – original draft, Writing – review & editing.

Declaration of Competing Interest

The authors declare that they have no known competing financial interests or personal relationships that could have appeared to influence the work reported in this paper.

Acknowledgments:

This work was supported by the National Science Centre (Poland) [grant number 2016/23/N/NZ9/02224]; the European Cooperation in Science and Technology (COST) organization in the framework of the EpiLipidNET CA19105 COST Action; the Excellence Initiative – Research University project of Gdańsk University of Technology (Poland); the FCT/MCT (Portugal); and

research units LAQV-REQUIMTE [grant number UIDB/50006/2020] and CESAM [grant number UIDP/50017/2020 + UIDB/50017/2020 + LA/P/0094/2020].

Appendix A. Supplementary data

Supplementary data to this article can be found online.

References

Andrews, J. S., Griffith, W. H., Mead, J. F., & Stein, R. A. (1960). Toxicity of air-oxidized soybean oil. *The Journal of Nutrition*, *70*(2), 199–210.

Awada, M., Soulage, C. O., Meynier, A., Debard, C., Plaisancié, P., Benoit, B., … Michalski, M. C. (2012). Dietary oxidized n-3 PUFA induce oxidative stress and inflammation: Role of intestinal absorption of 4-HHE and reactivity in intestinal cells. *Journal of Lipid Research*, *53*(10), 2069–2080. https://doi.org/10.1194/jlr.M026179

Baba, N., Mikami, Y., Shigeta, Y., Nakajima, S., & Matsuo, M. (1993). Hydrolysis of glycerophosphocholine hydroperoxide by phospholipase A2. *Bioscience, Biotechnology, and Biochemistry*, *51*(12), 2200–2201. https://doi.org/10.1271/bbb.57.2200

Baburina, I., & Jackowski, S. (1999). Cellular responses to excess phospholipid. *Journal of Biological Chemistry*, *274*(14), 9400–9408. https://doi.org/10.1074/jbc.274.14.9400

Baranowska, M., Koziara, Z., Suliborska, K., Chrzanowski, W., Wormstone, M., Namieśnik, J., & Bartoszek, A. (2021). Interactions between polyphenolic antioxidants quercetin and naringenin dictate the distinctive redox-related chemical and biological behaviour of their mixtures. *Scientific Reports*, *11*(1), 1–18. https://doi.org/10.1038/s41598-021-89314-0

Baranowska, M., Suliborska, K., Chrzanowski, W., Kusznierewicz, B., Namie, J., & Bartoszek, A. (2018). The relationship between standard reduction potentials of catechins and biological activities involved in redox control. *Redox Biology*, *17*, 355–366. https://doi.org/10.1016/j.redox.2018.05.005

Baranowska, M., Suliborska, K., Todorovic, V., Kusznierewicz, B., Chrzanowski, W., Sobajic, S., & Bartoszek, A. (2020). Interactions between bioactive components determine antioxidant, cytotoxic and nutrigenomic activity of cocoa powder extract. *Free Radical Biology and Medicine*, *154*, 48–61. https://doi.org/10.1016/j.freeradbiomed.2020.04.022

Bashllari, R., Molonia, M. S., Muscarà, C., Speciale, A., Wilde, P. J., Saija, A., & Cimino, F. (2020). Cyanidin-3-O-glucoside protects intestinal epithelial cells from palmitate-induced lipotoxicity. *Archives of Physiology and Biochemistry*, 1–8. https://doi.org/10.1080/13813455.2020.1828480

Beilstein, F., Carrière, V., Leturque, A., & Demignot, S. (2016). Characteristics and functions of lipid droplets and associated proteins in enterocytes. *Experimental Cell Research*, *340*(2), 172–179. https://doi.org/10.1016/j.yexcr.2015.09.018

Beisson, F., Tiss, A., Rivière, C., & Verger, R. (2000). Methods for lipase detection and assay: A critical review. *European Journal of Lipid Science and Technology*, *102*(2), 133–153. https://doi.org/10.1002/(sici)1438-9312(200002)102:2<133::aid-ejlt133>3.0.co;2-x

Birru, W. A., Warren, D. B., Ibrahim, A., Williams, H. D., Benameur, H., Porter, C. J. H., … Pouton, C. W. (2014). Digestion of phospholipids after secretion of bile into the duodenum changes the phase behavior of bile components. *Molecular Pharmaceutics*, *11*(8), 2825–2834. https://doi.org/10.1021/mp500193g

Blesso, C. N. (2015). Egg phospholipids and cardiovascular health. *Nutrients*, *7*(4), 2731–2747. https://doi.org/10.3390/nu7042731

Borgström, B. (1980). Importance of phospholipids, pancreatic phospholipase A2, and fatty acid for the digestion of dietary fat in vitro experiments enzymes. *Gastroenterology*, *78*, 954–962.

Brash, A. R. (1999). Lipoxygenases: Occurrence, functions, catalysis, and acquisition of substrate. *The Journal of Biological Chemistry*, *274*(34), 23679–23683.

Butler O'Connor, E. S., Mazerik, J. N., Cruff, J. P., Sherwani, S. I., Weis, B. K., Marsh, C. B., … Parinandi, N. L. (2010). Lipoxygenase-catalyzed phospholipid peroxidation: Preparation, purification, and characterization of phosphatidylinositol peroxides. In R. M. Uppu, S. N. Murthy, W. A. Pryor, & N. L. Parinandi (Eds.), *Free Radicals and Antioxidant Protocols. Methods in Molecular Biology (Methods and Protocols)* (2nd ed., pp. 387–401). Humana Press. https://doi.org/10.1007/978-1-60327-029-8

Catalá, A. (2012). Lipid peroxidation modifies the picture of membranes from the "Fluid Mosaic Model" to the "Lipid Whisker Model." *Biochimie*, *94*(1), 101–109.

https://doi.org/10.1016/j.biochi.2011.09.025
Catalá, A. (2015). Lipid peroxidation modifies the assembly of biological membranes “The Lipid Whisker Model.” *Frontiers in Physiology*, *5*(520), 1–4. https://doi.org/10.3389/fphys.2014.00520
Catalá, A., & Díaz, M. (2016). Editorial: Impact of lipid peroxidation on the physiology and pathophysiology of cell membranes. *Frontiers in Physiology*, *7*(423), 1–3. https://doi.org/10.3389/fphys.2016.00423
Catalán, V., Frühbeck, G., & Gómez-Ambrosi, J. (2018). Inflammatory and oxidative stress markers in skeletal muscle of obese subjects. In A. Marti del Moral & C. M. Aguilera (Eds.), *Obesity* (pp. 163–189). Academic Press. https://doi.org/10.1016/B978-0-12-812504-5.00008-8
Chen, D. W., Balagiannis, D. P., & Parker, J. K. (2019). Use of egg yolk phospholipids to generate chicken meat odorants. *Food Chemistry*, *286*, 71–77. https://doi.org/10.1016/j.foodchem.2019.01.184
Cui, L., & Decker, E. A. (2016). Phospholipids in foods: Prooxidants or antioxidants? *Journal of the Science of Food and Agriculture*, *96*(1), 18–31. https://doi.org/10.1002/jsfa.7320
Dennis, E. A., Cao, J., Hsu, Y.-H., Magrioti, V., & Kokotos, G. (2011). Phospholipase A2 enzymes: Physical structure, biological function, disease implication, chemical inhibition, and therapeutic intervention. *Chemical Reviewseviews*, *111*(10), 6130–6185. https://doi.org/10.1021/cr200085w.Phospholipase
Dittmer, J. C., & Lester, R. L. (1964). A simple, specific spray for the detection of phospholipids on thin-layer chromatograms. *Journal of Lipid Research*, *5*(1), 126–127.
Domínguez, R., Pateiro, M., Gagaoua, M., Barba, F. J., Zhang, W., & Lorenzo, J. M. (2019). A comprehensive review on lipid oxidation in meat and meat products. *Antioxidants*, *8*(10), 1–31. https://doi.org/10.3390/antiox8100429
Faizo, N., Narasimhulu, C. A., Forsman, A., Yooseph, S., & Parthasarathy, S. (2021). Peroxidized linoleic acid, 13-HPODE, alters gene expression profile in intestinal epithelial cells. *Foods*, *10*(2), 1–23. https://doi.org/10.3390/foods10020314
Fedi, A., Vitale, C., Ponschin, G., Ayehunie, S., Fato, M., & Scaglione, S. (2021). In vitro models replicating the human intestinal epithelium for absorption and metabolism studies: A systematic review. *Journal of Controlled Release*, *335*, 247–268. https://doi.org/10.1016/j.jconrel.2021.05.028
Fenaille, F., Mottier, P., Turesky, R. J., Ali, S., & Guy, P. A. (2001). Comparison of analytical techniques to quantify malondialdehyde in milk powders. *Journal of Chromatography A*, *921*(2), 237–245. https://doi.org/10.1016/S0021-9673(01)00883-4
Fruehwirth, S., Zehentner, S., Salim, M., Sterneder, S., Tiroch, J., Lieder, B., … Pignitter, M. (2020). In vitro digestion of grape seed oil inhibits phospholipid-regulating effects of oxidized lipids. *Biomolecules*, *10*(708), 1–20. https://doi.org/10.3390/biom10050708
Fruhwirth, G. O., Loidl, A., & Hermetter, A. (2007). Oxidized phospholipids: From molecular properties to disease. *Biochimica et Biophysica Acta - Molecular Basis of Disease*, *1772*(7), 718–736. https://doi.org/10.1016/j.bbadis.2007.04.009
Gilbraith, W. E., Carter, J. C., Adams, K. L., Booksh, K. S., & Ottaway, J. M. (2021). Improving prediction of peroxide value of edible oils using regularized regression models. *Molecules*, *26*(23), 1–20. https://doi.org/10.3390/molecules26237281
Girón-Calle, J., Schmid, P. C., & Schmid, H. H. O. (1997). Effects of oxidative stress on glycerolipid acyl turnover in rat hepatocytes. *Lipids*, *32*(9), 917–923. https://doi.org/10.1007/s11745-997-0118-9
Gładkowski, W., Chojnacka, A., Kiełbowicz, G., Trziszka, T., & Wawrzeńczyk, C. (2012). Isolation of pure phospholipid fraction from egg yolk. *Journal of the American Oil Chemists' Society*, *89*(1), 179–182. https://doi.org/10.1007/s11746-011-1893-x
Gotoh, N., Watanabe, H., Osato, R., Inagaki, K., Iwasawa, A., & Wada, S. (2006). Novel approach on the risk assessment of oxidized fats and oils for perspectives of food safety and quality. I. Oxidized fats and oils induces neurotoxicity relating pica behavior and hypoactivity. *Food and Chemical Toxicology*, *44*(4), 493–498. https://doi.org/10.1016/j.fct.2005.08.023
Grootveld, M., Percival, B. C., Leenders, J., & Wilson, P. B. (2020). Potential adverse public health effects afforded by the ingestion of dietary lipid oxidation product toxins: Significance of fried food sources. *Nutrients*, *12*(974), 1–49. https://doi.org/10.3390/nu12040974
Gulhane, M., Murray, L., Lourie, R., Tong, H., Sheng, Y. H., Wang, R., … Hasnain, S. Z. (2016). High fat diets induce colonic epithelial cell stress and inflammation that is reversed by IL-22. *Scientific Reports*, *6*, 1–17. https://doi.org/10.1038/srep28990
Gundermann, K. J., Gundermann, S., Drozdzik, M., & Mohan Prasad, V. G. (2016). Essential phospholipids in fatty liver: A scientific update. *Clinical and Experimental Gastroenterology*, *9*,

105–117. https://doi.org/10.2147/CEG.S96362
Gupta, A., Eral, H. B., Hatton, T. A., & Doyle, P. S. (2016). Nanoemulsions: Formation, properties and applications. *Soft Matter*, *12*(11), 2826–2841. https://doi.org/10.1039/c5sm02958a
Guyon, C., Meynier, A., & de Lamballerie, M. (2016). Protein and lipid oxidation in meat: A review with emphasis on high-pressure treatments. *Trends in Food Science and Technology*, *50*, 131–143. https://doi.org/10.1016/j.tifs.2016.01.026
Henning, R. J., Johnson, G. T., Coyle, J. P., & Harbison, R. D. (2017). Acrolein can cause cardiovascular disease: A review. *Cardiovascular Toxicology*, *17*(3), 227–236. https://doi.org/10.1007/s12012-016-9396-5
Igene, J. O., Pearson, A. M., Dugan, L. R., & Price, J. F. (1980). Role of triglycerides and phospholipids on development of rancidity in model meat systems during frozen storage. *Food Chemistry*, *5*(4), 263–276. https://doi.org/10.1016/0308-8146(80)90048-5
Jackson, V., & Penumetcha, M. (2019). Dietary oxidised lipids, health consequences and novel food technologies that thwart food lipid oxidation: an update. *International Journal of Food Science and Technology*, *54*(6), 1981–1988. https://doi.org/10.1111/ijfs.14058
Jacobsen, C., Paiva-Martins, F., Schwarz, K., & Bochkov, V. (2019). Lipid oxidation and antioxidants in food and nutrition. *European Journal of Lipid Science and Technology*, *121*(9), 1–1. https://doi.org/10.1002/ejlt.201900298
Jiang, K., Huang, C., Liu, F., Zheng, J., Ou, J., Zhao, D., & Ou, S. (2022). Origin and fate of acrolein in foods. *Foods*, *11*(13), 1–24. https://doi.org/10.3390/foods11131976
Jiménez-Rojo, N., Viguera, A. R., Collado, M. I., Sims, K. H., Constance, C., Hill, K., … Alonso, A. (2014). Sphingosine induces the aggregation of imine-containing peroxidized vesicles. *Biochimica et Biophysica Acta - Biomembranes*, *1838*(8), 2071–2077. https://doi.org/10.1016/j.bbamem.2014.04.028
Jittrepotch, N., Ushio, H., & Ohshima, T. (2006). Oxidative stabilities of triacylglycerol and phospholipid fractions of cooked Japanese sardine meat during low temperature storage. *Food Chemistry*, *99*(2), 360–367. https://doi.org/10.1016/j.foodchem.2005.08.002
Kambayashi, Y., Yamamoto, Y., & Nakan, M. (1998). Preferential hydrolysis of oxidized phosphatidylcholine in cholesterol-containing phosphatidylcholine liposome by phospholipase A2. *Biochemical and Biophysical Research Communications*, *245*(3), 705–708.
Kanner, J. (2007). Dietary advanced lipid oxidation endproducts are risk factors to human health. *Molecular Nutrition & Food Research*, *51*(9), 1094–1101. https://doi.org/10.1002/mnfr.200600303
Keewan, E., Narasimhulu, C. A., Rohr, M., Hamid, S., & Parthasarathy, S. (2020). Are fried foods unhealthy? The dietary peroxidized fatty acid, 13-HPODE, induces intestinal inflammation in vitro and in vivo. *Antioxidants*, *9*(10), 1–17. https://doi.org/10.3390/antiox9100926
Kölbel, K., Weininger, U., Ihling, C., Mrestani-Klaus, C., & Ulbrich-Hofmann, R. (2015). Native state dynamics affects the folding transition of porcine pancreatic phospholipase A2. *Biophysical Chemistry*, *206*, 12–21. https://doi.org/10.1016/j.bpc.2015.06.007
Krishna, G., & Gopalakrishnan, G. (2016). Alternative in vitro models for safety and toxicity evaluation of nutraceuticals. In R. C. Gupta (Ed.), *Nutraceuticals* (pp. 355–386). Academic Press. https://doi.org/10.1016/B978-0-12-802147-7.00027-9
Küllenberg de Gaudry, D., Taylor, L. a, Schneider, M., & Massing, U. (2012). Health effects of dietary phospholipids. *Lipids in Health and Disease*, *11*(1), 1–16. https://doi.org/10.1186/1476-511X-11-3
Kupper, S., Kłosowska-Chomiczewska, I., & Szumała, P. (2017). Collagen and hyaluronic acid hydrogel in water-in-oil microemulsion delivery systems. *Carbohydrate Polymers*, *175*, 347–354. https://doi.org/10.1016/j.carbpol.2017.08.010
Lian, C. Y., Zhai, Z. Z., Li, Z. F., & Wang, L. (2020). High fat diet-triggered non-alcoholic fatty liver disease: A review of proposed mechanisms. *Chemico-Biological Interactions*, *330*, 1–15. https://doi.org/10.1016/j.cbi.2020.109199
Lipke, K., Kubis-Kubiak, A., & Piwowar, A. (2022). Molecular mechanism of lipotoxicity as an interesting aspect in the development of pathological states - Current view of knowledge. *Cells*, *11*(844), 1–34. https://doi.org/10.3390/cells11050844
Lísa, M., Cífková, E., & Holčapek, M. (2011). Lipidomic profiling of biological tissues using off-line two-dimensional high-performance liquid chromatography-mass spectrometry. *Journal of Chromatography A*, *1218*(31), 5146–5156. https://doi.org/10.1016/j.chroma.2011.05.081
Listenberger, L. L., & Brown, D. A. (2007). Fluorescent detection of lipid droplets and associated proteins. *Current Protocols in Cell Biology*, *35*(1), 24.2.1-24.2.11.
Litvinko, N. M., Skorostetskaya, L. A., & Gerlovsky, D. O. (2018). The interaction of phospholipase A2 with oxidized phospholipids at the lipid-water surface with different structural organization.

Chemistry and Physics of Lipids, *211*, 44–51. https://doi.org/10.1016/j.chemphyslip.2017.10.010
Macierzanka, A., Torcello-Gómez, A., Jungnickel, C., & Maldonado-Valderrama, J. (2019). Bile salts in digestion and transport of lipids. *Advances in Colloid and Interface Science*, *274*, 1–17. https://doi.org/10.1016/j.cis.2019.102045
Maldonado-Valderrama, J., Wilde, P., MacIerzanka, A., & MacKie, A. (2011). The role of bile salts in digestion. *Advances in Colloid and Interface Science*, *165*(1), 36–46. https://doi.org/10.1016/j.cis.2010.12.002
Martin-Rubio, A. S., Sopelana, P., Ibargoitia, M. L., & Guillén, M. D. (2021). 1H NMR study of the in vitro digestion of highly oxidized soybean oil and the effect of the presence of ovalbumin. *Foods*, *10*(7), 1–26. https://doi.org/10.3390/foods10071573
Martínez-Maqueda, D., Miralles, B., & Recio, I. (2015). HT29 cell line. In K. Verhoeckx, P. Cotter, I. López-Expósito, C. Kleiveland, T. Lea, A. Mackie, … H. Wichers (Eds.), *The Impact of Food Bioactives on Health: In Vitro and Ex Vivo Models* (1st ed., pp. 113–124). Springer Cham. https://doi.org/10.1007/978-3-319-16104-4
Meca, A. D., Turcu-Stiolica, A., Stanciulescu, E. C., Andrei, A. M., Nitu, F. M., Banita, I. M., … Pisoschi, C. G. (2021). Variations of serum oxidative stress biomarkers under first-line antituberculosis treatment: A pilot study. *Journal of Personalized Medicine*, *11*(2), 1–10. https://doi.org/10.3390/jpm11020112
Meyuhas, D., Bor, A., Pinchuk, I., Kaplun, A., Talmon, Y., Kozlov, M. M., & Lichtenberg, D. (1997). Effect of ionic strength on the self-assembly in mixtures of phosphatidylcholine and sodium cholate. *Journal of Colloid and Interface Science*, *188*(2), 351–362.
Montgomery, M. K., De Nardo, W., & Watt, M. J. (2019). Impact of lipotoxicity on tissue “cross talk” and metabolic regulation. *Physiology*, *34*(2), 134–149. https://doi.org/10.1152/physiol.00037.2018
Nguyen, T. T., Ung, T. T., Kim, N. H., & Jung, Y. Do. (2018). Role of bile acids in colonic carcinogenesis. *World Journal of Clinical Cases*, *6*(13), 577–588. https://doi.org/10.1007/BF01734247
Nicolson, G. L., & Ash, M. E. (2014). Lipid Replacement Therapy: A natural medicine approach to replacing damaged lipids in cellular membranes and organelles and restoring function. *Biochimica et Biophysica Acta - Biomembranes*, *1838*(6), 1657–1679. https://doi.org/10.1016/j.bbamem.2013.11.010
Nieva-Echevarría, B., Goicoechea, E., & Guillén, M. D. (2018). Food lipid oxidation under gastrointestinal digestion conditions: A review. *Critical Reviews in Food Science and Nutrition*, *60*(3), 1–18. https://doi.org/10.1080/10408398.2018.1538931
Palusinska-Szysz, M., Kania, M., Turska-Szewczuk, A., & Danikiewicz, W. (2014). Identification of unusual phospholipid fatty acyl compositions of Acanthamoeba castellanii. *PloS One*, *9*(7), e101243. https://doi.org/10.1371/journal.pone.0101243
Pamplona, R. (2008). Membrane phospholipids, lipoxidative damage and molecular integrity: A causal role in aging and longevity. *Biochimica et Biophysica Acta - Bioenergetics*, *1777*(10), 1249–1262. https://doi.org/10.1016/j.bbabio.2008.07.003
Parchem, K., Kusznierewicz, B., Chmiel, T., Maciołek, P., & Bartoszek, A. (2019). Profiling and qualitative assessment of enzymatically and thermally oxidized egg yolk phospholipids using a two-step HPLC protocol. *Journal of the American Oil Chemists' Society*, *96*(6), 693–706.
Parchem, K., Sasson, S., Ferreri, C., & Bartoszek, A. (2019). Qualitative analysis of phospholipids and their oxidised derivatives–used techniques and examples of their applications related to lipidomic research and food analysis. *Free Radical Research*, *53*(sup1), 1068–1100. https://doi.org/10.1080/10715762.2019.1657573
Penumetcha, M., Khan, N., & Parthasarathy, S. (2000). Dietary oxidized fatty acids: an atherogenic risk? *Journal of Lipid Research*, *41*(9), 1473–1480.
Riethorst, D., Baatsen, P., Remijn, C., Mitra, A., Tack, J., Brouwers, J., & Augustijns, P. (2016). An in-depth view into human intestinal fluid colloids: Intersubject variability in relation to composition. *Molecular Pharmaceutics*, *13*, 3484–3493. https://doi.org/10.1021/acs.molpharmaceut.6b00496
Rosignoli, P., Fabiani, R., De Bartolomeo, A., Fuccelli, R., Pelli, M. A., & Morozzi, G. (2008). Genotoxic effect of bile acids on human normal and tumour colon cells and protection by dietary antioxidants and butyrate. *European Journal of Nutrition*, *47*(6), 301–309. https://doi.org/10.1007/s00394-008-0725-8
Sasson, S. (2017). Nutrient overload, lipid peroxidation and pancreatic beta cell function. *Free Radical Biology and Medicine*, *111*, 102–109. https://doi.org/10.1016/j.freeradbiomed.2016.09.003
Tan, Y., Qi, J., Lu, Y., Hu, F., Yin, Z., & Wu, W. (2013). Lecithin in mixed micelles attenuates the cytotoxicity of bile salts in Caco-2 cells. *Toxicology in Vitro*, *27*, 714–720.

https://doi.org/10.1016/j.tiv.2012.11.018
Tsunada, S., Iwakiri, R., Noda, T., Fujimoto, K., Fuseler, J., Rhoads, C. A., & Aw, T. Y. (2003). Chronic exposure to subtoxic levels of peroxidized lipids suppresses mucosal cell turnover in rat small intestine and reversal by glutathione. *Digestive Diseases and Sciences*, *48*(1), 210–222. https://doi.org/10.1023/A:1021775524062
Van Rijn, J. M., Van Hoesel, M., De Heus, C., Van Vugt, A. H. M., Klumperman, J., Nieuwenhuis, E. E. S., … Middendorp, S. (2019). DGAT2 partially compensates for lipid-induced ER stress in human DGAT1-deficient intestinal stem cells. *Journal of Lipid Research*, *60*(10), 1787–1800. https://doi.org/10.1194/jlr.M094201
Vieira, S. A., Zhang, G., & Decker, E. A. (2017). Biological implications of lipid oxidation products. *JAOCS, Journal of the American Oil Chemists' Society*, *94*(3), 339–351. https://doi.org/10.1007/s11746-017-2958-2
Wang, T., Gotoh, Y., Jennings, M. H. O., & Rhoads, C. A. N. N. (2000). Lipid hydroperoxide-induced apoptosis in human colonic CaCo-2 cells is associated with an early loss of cellular redox balance. *The FASEB Journal*, *14*(11), 1567–1576.
Wang, T. Y., Libardo, M. D. J., Angeles-Boza, A. M., & Pellois, J. P. (2017). Membrane oxidation in cell delivery and cell killing applications. *ACS Chemical Biology*, *12*(5), 1170–1182. https://doi.org/10.1021/acschembio.7b00237
Wąsowicz, E., Gramza, A., Hęś, M., Jeleń, H. H., Korczak, J., Małecka, M., … Zawirska-Wojtasiak, R. (2004). Oxidation of lipids in foods. *Polish Journal of Food and Nutrition Science*, *13*(54), 87–100.
Zierenberg, O., & Grundy, S. M. (1982). Intestinal absorption of polyenephosphatidylcholine in man. *Journal of Lipid Research*, *23*(8), 1136–1142. https://doi.org/10.1016/s0022-2275(20)38050-0